Carbon/nitrogen interactions in European forests and semi-natural vegetation. Part II: Untangling climatic, edaphic, management and nitrogen deposition effects on carbon sequestration potentials

Chris R. Flechard[1], Marcel van Oijen[2], David R. Cameron[2], Wim de Vries[3], Andreas Ibrom[4], Nina Buchmann[5], Nancy B. Dise[2], Ivan A. Janssens[6], Johan Neirynck[7], Leonardo Montagnani[8,9], Andrej Varlagin[10], Denis Loustau[11], Arnaud Legout[12], Klaudia Ziemblińska[13], Marc Aubinet[14], Mika Aurela[15], Bogdan H. Chojnicki[16], Julia Drewer[2], Werner Eugster[5], André-Jean Francez[17], Radosław Juszczak[16], Barbara Kitzler[18], Werner L. Kutsch[19], Annalea Lohila[20,15], Bernard Longdoz[21], Giorgio Matteucci[22], Virginie Moreaux[11,23], Albrecht Neftel[24], Janusz Olejnik[13,25], Maria J. Sanz[26], Jan Siemens[27], Timo Vesala[20,28], Caroline Vincke[29], Eiko Nemitz[2], Sophie Zechmeister-Boltenstern[30], Klaus Butterbach-Bahl[31], Ute M. Skiba[2] and Mark A. Sutton[2]

[1] Institut National de la Recherche Agronomique (INRA), UMR 1069 SAS, 65 rue de Saint-Brieuc, F-35042 Rennes, France
[2] Centre for Ecology and Hydrology (CEH), Bush Estate, Penicuik, EH26 0QB, UK
[3] Wageningen University and Research, Environmental Systems Analysis Group, PO Box 47, NL-6700 AA Wageningen, the Netherlands
[4] Department of Environmental Engineering, Technical University of Denmark, Bygningstorvet, DK-2800 Kgs. Lyngby, Denmark
[5] Department of Environmental Systems Science, Institute of Agricultural Sciences, ETH Zurich, LFW C56, Universitatstr. 2, CH-8092 Zurich, Switzerland
[6] Centre of Excellence PLECO (Plant and Vegetation Ecology), Department of Biology, University of Antwerp, BE-2610 Wilrijk, Belgium
[7] Research Institute for Nature and Forest (INBO), Gaverstraat 35, BE-9500 Geraardsbergen, Belgium
[8] Forest Services, Autonomous Province of Bolzano, Via Brennero 6, I-39100 Bolzano, Italy
[9] Faculty of Science and Technology, Free University of Bolzano, Piazza Università 5, I-39100 Bolzano, Italy
[10] A.N. Severtsov Institute of Ecology and Evolution, Russian Academy of Sciences, 119071, Leninsky pr.33, Moscow, Russia
[11] Institut National de la Recherche Agronomique (INRA), UMR 1391 ISPA, F-33140 Villenave d'Ornon, France
[12] INRA, BEF, F-54000 Nancy, France
[13] Department of Meteorology, Poznań University of Life Sciences, Piątkowska 94, 60-649 Poznań, Poland
[14] TERRA Teaching and Research Centre, Gembloux Agro-Bio Tech, University of Liège, Belgium
[15] Finnish Meteorological Institute, Climate System Research, PL 503, FI-00101, Helsinki, Finland
[16] Laboratory of Bioclimatology, Department of Ecology and Environmental Protection, Poznan University of Life Sciences, Piatkowska 94, 60-649 Poznan, Poland
[17] University of Rennes, CNRS, UMR 6553 ECOBIO, Campus de Beaulieu, 263 avenue du Général Leclerc, F-35042 Rennes cedex, France
[18] Federal Research and Training Centre for Forests, Natural Hazards and Landscape, Seckendorff-Gudent-Weg 8, A-1131 Vienna, Austria
[19] Integrated Carbon Observation System (ICOS ERIC) Head Office, Erik Palménin aukio 1, FI-00560 Helsinki, Finland
[20] Institute for Atmospheric and Earth System Research/Physics, Faculty of Science, POBox 68, FI-00014 University of Helsinki, Finland
[21] Gembloux Agro-Bio Tech, Axe Echanges Ecosystèmes Atmosphère, 8, Avenue de la Faculté, BE-5030 Gembloux, Belgium
[22] National Research Council of Italy, Institute for Agriculture and Forestry Systems in the Mediterranean (CNR-ISAFOM), Via Patacca, 85 I-80056 Ercolano (NA), Italy
[23] Université Grenoble Alpes, CNRS, IGE, F-38000 Grenoble, France
[24] NRE, Oberwohlenstrasse 27, CH-3033 Wohlen b. Bern, Switzerland
[25] Department of Matter and Energy Fluxes, Global Change Research Centre, AS CR, v.v.i. Belidla 986/4a, 603 00 Brno, Czech Republic
[26] Basque Centre for Climate Change (BC3), Scientific Park, Sede Building, s/n Leioa, Bizkaia, Spain
[27] Institute of Soil Science and Soil Conservation, iFZ Research Centre for Biosystems, Land Use and Nutrition, Justus Liebig University Giessen, Heinrich-Buff-Ring 26-32, D-35392 Giessen, Germany
[28] Institute for Atmospheric and Earth System Research/Forest Sciences, Faculty of Agriculture and Forestry, PO. Box 27, FI-00014 University of Helsinki, Finland
[29] Earth and Life Institute (Environmental sciences), Université catholique de Louvain, Louvain-la-Neuve, Belgium.
[30] Institute of Soil Research, Department of Forest and Soil Sciences, University of Natural Resources and Life Sciences Vienna, Peter Jordan Str. 82, A-1190 Vienna, Austria
[31] Karlsruhe Institute of Technology (KIT), Institute of Meteorology and Climate Research, Atmospheric Environmental Research (IMK-IFU), Kreuzeckbahnstr. 19, D-82467 Garmisch-Partenkirchen, Germany

Correspondence to: Chris R. Flechard (christophe.flechard@inra.fr)

60   **Abstract**. The effects of atmospheric nitrogen deposition (N_{dep}) on carbon (C) sequestration in forests have often been assessed by relating differences in productivity to spatial variations of N_{dep} across a large geographic domain. These correlations generally suffer from covariation of other confounding variables related to climate and other growth-limiting factors, as well as large uncertainties in total (dry + wet) reactive nitrogen (N_r) deposition. We propose a methodology for untangling the effects of N_{dep} from those of meteorological variables, soil water retention capacity and stand age, using a

65   mechanistic forest growth model in combination with eddy covariance CO_2 exchange fluxes from a Europe-wide network of forest flux towers. Total N_r deposition rates were estimated from local measurements as far as possible. The forest data were compared with data from natural or semi-natural, non-woody vegetation sites. The carbon sequestration response of forests to nitrogen deposition (dC/dN) was estimated after accounting for the effects of the co-correlates by means of a meta-modelling standardization procedure, which resulted in a reduction by a factor of about 2 of the uncorrected, apparent dC/dN value. This

70   model-enhanced analysis of the C and N_{dep} flux observations at the scale of the European network suggests a mean overall dC/dN response of forest lifetime C sequestration to N_{dep} of the order of 40–50 g (C) g^{-1} (N), which is slightly larger but not significantly different from the range of estimates published in the most recent reviews. Importantly, patterns of gross primary and net ecosystem productivity versus N_{dep} were non-linear, with no further responses at high N_{dep} levels ($N_{dep} > 2.5$– 3 g (N) m^{-2} yr^{-1}) partly due to large ecosystem N losses by leaching and gaseous emissions. The reduced increase in

75   productivity per unit N deposited at high N_{dep} levels implies that the forecast increased N_r emissions and increased N_{dep} levels in large areas of Asia may not positively impact the continent's forest CO_2 sink. The large level of unexplained variability in observed carbon sequestration efficiency (CSE) across sites further adds to the uncertainty in the dC/dN response.

1 Introduction

Atmospheric reactive nitrogen (N_r) deposition (N_{dep}) has often been suggested to be a major driver of the large forest carbon

80   (C) sink observed in the Northern Hemisphere (Reay et al., 2008; Ciais et al., 2013), but this view has been challenged, both in temperate (Nadelhoffer et al., 1999; Lovett et al., 2013) and in boreal regions (Gundale et al., 2014). In principle, there is a general consensus that N limitation significantly reduces net primary productivity (NPP) (LeBauer and Treseder, 2008; Zaehle and Dalmonech, 2011; Finzi et al., 2007). However, the measure of carbon sequestration is not the NPP, but the long term net ecosystem carbon balance (NECB; Chapin et al., 2006) or the net biome productivity at a large spatial scale (NBP;

85   Schulze et al., 2010), whereby heterotrophic respiration (R_{het}) and all other C losses, including exported wood products and other disturbances over a forest lifetime, reduce the fraction of photosynthesized C (gross primary production, GPP) that is actually sequestered in the ecosystem.

There is considerable debate as to the magnitude of the "fertilisation" role that atmospheric N_r deposition may play on forest carbon balance, as illustrated by the controversy over the study by Magnani et al. (2007) and subsequent comments by

90   Högberg (2007), De Schrijver et al. (2008), Sutton et al. (2008), and others. Estimates of the dC/dN response (mass C stored in the ecosystem per mass atmospheric N deposited) vary across these studies over an order of magnitude, from 30–70 g (C) g^{-1} (N) (de Vries et al., 2008; Sutton et al., 2008; Högberg, 2012), to 121 (Dezi et al., 2010), to 200–725 (Magnani et al., 2007, 2008). Recent reviews have suggested mean dC/dN responses generally well below 100 g (C) g^{-1} (N), ranging from 61– 98 for US forests (Thomas et al., 2010), 35–65 (Erisman et al., 2011; Butterbach-Bahl and Gundersen, 2011), 16–33 (Liu and

95   Greaver, 2009), 5–75 (mid-range 20–40) for European forests and heathlands (de Vries et al., 2009), and down to 13–14 in temperate and boreal forests (aboveground woody biomass only; Schulte-Uebbing and de Vries, 2018), and 5–25 for forests globally (de Vries et al., 2014).

A better understanding of processes controlling the dC/dN response is key to predicting the magnitude of the forest C sink under global change in response to changing patterns of reactive nitrogen (N_r) emissions and deposition (Fowler et al., 2015).

100   The question of the allocation and fate of the deposited nitrogen appears to be crucial; N_r deposition plays a significant role in promoting the carbon sink strength only if N is stored in woody tissues with high C/N ratios (>200−500) and long turnover times, as opposed to soil organic matter (SOM) with C/N ratios that are an order of magnitude smaller (de Vries et al., 2008). Nadelhoffer et al. (1999) argued on the basis of a review of ^{15}N tracer experiments that soil, rather than tree biomass, was the primary sink for the added nitrogen in temperate forests; and at sites with elevated N inputs, increasingly large fractions were

105   lost as nitrate (NO_3^-) leaching. Lovett et al. (2013) found in north-eastern US forests that added N increased C and N stocks and the C/N ratio in the forest floor, but did not increase woody biomass or aboveground NPP.

Atmospheric N_r deposition is rarely the dominant source of N supply for forests and semi-natural vegetation. Ecosystem internal turnover (e.g. leaf fall and subsequent decomposition of leaf litter) and mineralization of SOM provide annually larger amounts of mineral N than N_{dep} (although ultimately, over pedogenic time scales much of the N contained in SOM is

110   of atmospheric origin). In addition, resorption mechanisms help conserve within the tree the externally acquired N (and other nutrients), whereby N is re-translocated from senescing leaves to other growing parts of the tree, prior to leaf shedding, with resorption efficiencies of potentially up to 70% and larger at N-poor sites than at N-saturated sites (Vergutz et al., 2012; Wang et al., 2013). Biological N_2 fixation can also be significant in forests (Vitousek et al., 2002). Högberg (2012) showed for eleven European forest sites that N_r deposition was a relatively small fraction (13−14% on average) of the total N supply,

115   which was dominated by SOM mineralization (up to 15−20 g (N) m^{-2} yr^{-1}). He further argued that there may be a correlation between soil fertility (of which the natural N supply by mineralization is an indicator) and N_r deposition, since historically human populations have tended to develop settlements in areas of favourable edaphic conditions, in which over time agriculture, industry and population intensified, leading to increased emissions and deposition. Thus, an apparent effect of ambient N_{dep} on current net ecosystem productivity (NEP) levels could also be related to the legacy of more than a century of

120   N_r deposition on a modified internal ecosystem cycle.

Some previous estimates of forest dC/dN response obtained by meta-analyses of NEP or NECB across a geographic gradient did not account for the major drivers of plant growth apart from nitrogen. These include climate (precipitation, temperature, photosynthetically active radiation), soil physical and chemical properties (e.g. soil drainage, depth, and water holding capacity, nutrients, pH), site history and land use. Using univariate statistics such as simple regressions of NECB as a

125   function of N_r deposition is flawed if N_r deposition is co-correlated with any of these other drivers (Fleischer et al., 2013), as is usually the case in spatial gradient survey analyses across a wide geographic domain. This is because all of the variability in ecosystem C sequestration across the physical space is only allowed to be explained by one factor, N_r deposition. For example, Sutton et al. (2008) showed (using forest ecosystem modelling) that the apparently large dC/dN slope in the dataset of Magnani et al. (2007) was reduced by a factor of 2−3 when accounting for climatic differences between sites, i.e. when co-

130   varying limitations in (photosynthetic) energy and water were factored out.

Similarly, ignoring the growth stage (forest age) and the effects of management (thinning) in the analysis introduces additional uncertainty in the estimated dC/dN response. Contrasting C cycling patterns and different N use efficiencies are expected between young and mature forests. Nutrient demand is highest in the early stages of forest development (especially pole stage); a recently planted forest becomes a net C sink only after a few decades, while at maturity NPP and NEP may or

135   may not decrease, depending on a shift in the balance between autotrophic and heterotrophic respiration (R_{aut} and R_{het}, respectively) and GPP (Odum, 1969; Besnard et al., 2018). Thinning can initially increase ecosystem respiration by increasing litter and SOM stocks and reducing NPP in the short term, and some biomass can be exported (tree trunks), but the ultimate effect after a year or two is to boost forest growth as thinning indirectly increases nutrient availability at the tree level by reducing plant−plant competition. Thus, the frequency and intensity of thinning will also affect long-term or lifetime

140   NECB. Severe storms may have a similar effect.

Altogether, these complex interactions mean that it is far from a simple task to untangle the N_r deposition effect on ecosystem C sequestration from the impacts of climatic, edaphic and management factors, when analysing data from diverse monitoring sites situated over a large geographic area. This is in contrast to fertilisation experiments, where the N effect can be quantified

with all other variables being equal between manipulation plots, although their results are only valid for the conditions at the

145 specific location where the experiment has been performed (Schulte-Uebbing and de Vries, 2018). There are also potentially large uncertainties in the C and N flux measurements or model estimates used to calculate a dC/dN response. In the companion paper (Flechard et al., 2019), we presented – and discussed uncertainties in – plausible estimates of C and N budgets of 40 forests and natural or semi-natural ecosystems covering the main climatic zones of Europe (from Mediterranean to temperate to boreal, from oceanic to continental). The NEP budgets were based on multi-annual eddy

150 covariance (EC) datasets following well-established protocols, and in order to better constrain the N budgets, specific local measurements of dry and wet N_r deposition were made. Nitrogen losses by leaching and gaseous emissions were estimated by a combination of measurements and modelling. The data showed that observation-based GPP and NEP peaked at sites with N_{dep} of the order of 2–2.5 g (N) m^{-2} yr^{-1}, but decreased above that, and that increasingly large N_r losses occurred at larger N_{dep} levels, implying that the net dC/dN response was likely non-linear, possibly due to the onset of N saturation. The data also

155 showed that at the scale of the European CarboEurope IP flux tower network, nitrogen deposition was not independent of climate, but peaked in mid-range for both mean annual temperature and precipitation, which geographically corresponds to mid-latitude Central-Western Europe, where climate is most conducive to forest productivity and growth.

In the present paper, we further the analysis of the same observational datasets through forest ecosystem modelling, with the objective of isolating the N_r deposition impact on forest productivity and C sequestration potential from the parallel effects of

160 climate, soil water retention, and forest age and management. A mechanistic modelling framework, driven by environmental forcings, inputs, growth limitations, internal cycling and losses, was required to untangle the relationships in measurement data, because the observed dependence of N_r deposition on climate, combined with the large diversity but limited number of flux observation sites, restricted the applicability and validity of multivariate statistical methods. We describe a methodology to derive, through meta-modelling, standardization factors for observation-based forest productivity metrics, in order to factor

165 out the part of variance that was caused by influences other than N_r deposition (climate, soil, stand age). Further, we examine patterns of C and N use efficiency both at the decadal time scale of flux towers and over the lifetime of forests.

2 Materials and methods

2.1 Carbon and nitrogen datasets from flux tower sites

Ecosystem-scale carbon fluxes and atmospheric nitrogen deposition data were estimated at 31 European forests (six

170 deciduous broadleaf forests, DBF; 18 coniferous evergreen needleleaf forests, ENF, of which seven spruce-dominated and eleven pine-dominated; two mixed needleleaf/broadleaf forests, MF; five Mediterranean evergreen broadleaf forests, EBF) and nine short natural or semi-natural (SN) vegetation sites (wetlands, peatlands, unimproved and upland grasslands). The measurements were made mostly as part of the CarboEurope Integrated Project (CEIP, 2004–2008) and the parallel NitroEurope Integrated Project (NEU, 2006–2011). In the following we often adopted the terminology «*observation-based*»

175 rather than simply «*measured*», to reflect the fact many variables such as e.g. GPP or soil carbon pools rely on various assumptions or even empirical models for their estimation on the basis of measured data. For convenience in this paper, we use the following sign convention for CO_2 fluxes: GPP and R_{eco} are both positive, while NEP is positive for a net sink (a C gain from an ecosystem perspective) and negative for a net source.

The general characteristics of the observation sites (coordinates, dominant vegetation, forest stand age and height,

180 temperature and precipitation, N_{dep}, inter-annual mean C fluxes) are provided in Table S1 of the Supplement. The sites, measurement methods and data sources were described in more detail in the companion paper (Flechard et al., 2019); for additional information on vegetation, soils, C and N flux results and budgets, and their variability and uncertainties across the network, the reader is referred to that paper and the accompanying supplement. Briefly, the C datasets include multi-annual mean estimates of NEP, GPP and R_{eco} (total ecosystem respiration) based on 10–20 Hz EC measurements, post-processing,

185   spectral and other corrections, flux partitioning and empirical gap-filling (e.g. Lee et al., 2004; Aubinet et al., 2000; Falge et al., 2001; Reichstein et al., 2005; Lasslop et al., 2010). The fully analysed, validated, gap-filled and partitioned inter-annual mean CO_2 fluxes (NEP, GPP, R_{eco}), as well as the meteorological data used as ecosystem model inputs (Sect. 2.2), were retrieved from the European Fluxes Database Cluster (2012) and the NEU (2013) database. Dry deposition of reactive nitrogen was estimated by measuring at each site ambient concentrations of the dominant gas-phase (NH_3, HNO_3, NO_2) and

190   aerosol phase (NH_4^+, NO_3^-) N_r concentrations (data available from the NitroEurope database; NEU, 2013), and applying four different inferential models to the concentration and micro-meteorological data, as described in Flechard et al. (2011). Wet deposition was measured using bulk precipitation samplers (NEU, 2013, with additional data retrieved from national monitoring networks and from the EMEP chemical transport model (Simpson et al., 2012).

2.2 Modelling of forest C and N fluxes and pools

195   ### 2.2.1 Calibration and implementation of the BASFOR model

The BASic FORest model (BASFOR) is a deterministic forest ecosystem model that simulates the growth (from planting) and the biogeochemistry of temperate deciduous and coniferous even-aged stands (van Oijen et al., 2005). A description of the model is given in BASFOR (2016) and Cameron et al. (2018), and details on model implementation and a basic assessment of model performance in Flechard et al. (2019). Briefly, the C, N and water cycles are simulated at a daily time

200   step at the forest ecosystem scale (1-D model), in interaction with the soil and climate environments and constrained by management (pruning and thinning). Carbon and nitrogen pools are simulated in the different ecosystem compartments (tree stems, branches, leaves and roots, litter layers and SOM with fast and slow turnover), which are inter-connected by internal flows and transformations (e.g. SOM mineralization, nitrogen retranslocation). Carbon, nitrogen and water enter the ecosystem from the atmosphere (photosynthesis, N_r deposition, rainfall). Mineral nitrogen is taken up from the soil by tree

205   roots; C and N return to the litter and soil pools upon senescence of leaves, branches and roots, and also when trees are pruned or thinned. Losses of C occur through autotrophic (root and shoot) respiration and microbial decomposition into CO_2 of litter and SOM (heterotrophic respiration); losses of N occur through nitrate leaching below the root zone and soil emissions to the atmosphere of nitric oxide (NO) and nitrous oxide (N_2O). The water balance is constrained by incoming rainfall, soil water holding capacity, and evapotranspiration simulated by the Penman equation. Table 1 provides a summary

210   of model state variables, inputs and outputs, as well as the descriptions of other observation-based variables used in the study. For the purposes of this study, the model was calibrated through a multiple site Bayesian calibration (BC) procedure, applied to three groups of plant functional types (PFT), based on C/N/H_2O flux and pool data from the CEIP/NEU databases. A total of 22 sites were calibrated, including deciduous broadleaf forests (DB1-6), evergreen needleleaf forests ENF-spruce (EN1-7), and ENF-pine (EN8-18) (see Cameron et al., 2018). The model parameters were calibrated generically within each PFT

215   group, i.e. they were not optimized or adjusted individually for each observation site.
As a first step, baseline BASFOR runs were produced for all 31 forest sites of the network, including even stands for which the model was not calibrated, such as Mediterranean evergreen broadleaf (EB1 through EB5) and mixed deciduous/coniferous (MF1, MF2), to test the predictive capacity of the model beyond its calibration range (see Fig. 6 in Flechard et al., 2019). For the analyses and scenarios presented hereafter, these seven uncalibrated sites were removed from

220   the dataset, as were two additional sites: EN9 and EN12 (EN9 because this agrosilvopastoral ecosystem called «dehesa» has a very low tree density (70 trees ha^{-1}; Tables S1-S2 in the Supplement to Flechard et al., 2019) and is otherwise essentially dry grassland for much of the surface area, which BASFOR cannot simulate; EN12 because this was a very young plantation at the time of the measurements, also with a very large fraction of measured NEP from non-woody biomass). All the conclusions from BASFOR meta-modelling are drawn from the remaining 22 deciduous, pine and spruce stands.

225   *{Insert Table 1 here}*

2.2.2 Modelling time frames

In the companion paper (Flechard et al., 2019), C and N budgets were estimated primarily on the basis of ecosystem measurements and for the time horizon of the CEIP and NEU projects (2004–2010). In this paper, BASFOR simulations of the C and N budgets for the 22 forest sites were considered both i) over the most recent 5-year period (around the time of CEIP/NEU) which did not include any thinning event and started at least 3 years after the last thinning event (referred to hereafter as «5-yr»); and ii) over the whole time span since forest establishment, referred to here as «lifetime», which ranged from 30 to 190 years across the network and reflected the age of the stand at the time of the CEIP/NEU projects. Note that the term «lifetime» in this context was not used to represent the expected age of senescence or harvest.

On the one hand, the short term (5-yr) simulations were made to evaluate cases where no disturbance by management impacted fluxes and pools over a recent period, whatever the age of the stands at the time of the C and N flux measurements (ca 2000–2010). On the other hand, the lifetime simulations represent the time-integrated flux and pool history since planting, which reflects the long-term C sequestration (NECB) potential, controlled by the cumulative impact of management (thinning), increasing atmospheric CO_2 mixing ratio, and changing N_r deposition over the last few decades. Thinning modifies the canopy structure and therefore light, water and nutrient availability for the trees, reduces the LAI momentarily, and in theory the left-over additional organic residues (branches and leaves) could increase heterotrophic respiration and affect the NEP. However, the impact of the disturbance on NEP and R_{eco} is expected to be small and short-lived (Granier et al., 2008), and a 3-year wait after the last thinning event appears to be reasonable for the modelling. The 5-yr data should in theory reflect the C/N flux observations, although there were a few recorded thinning events during the CEIP/NEU measurement period, and the thinning sequences used as inputs to the model were reconstructed and thus not necessarily accurate (Table S2 and Fig. S5 in Supplement to Flechard et al., 2019).

2.2.3 Modelled carbon sequestration efficiency (CSE) and nitrogen use efficiency (NUE)

For both C and N, we define modelled indicators of ecosystem retention efficiency relative to a potential input level, which corresponds to the total C or N supply, calculated over both 5-yr (no thinning) and lifetime horizons to contrast short-term and long-term patterns. For C sequestration, the relevant terms are the temporal changes in carbon stocks in leaves, branches and stems (CLBS), roots (CR), soil organic matter (CSOM), and litter layers (CLITT), and the C export of woody biomass (CEXP), relative to the available incoming C from gross photosynthesis (GPP). We thus define the carbon sequestration efficiency (CSE) as the ratio of either modelled 5-yr NEP, or modelled lifetime NECB, to modelled GPP in a given environment, constrained by climate, nitrogen availability and other factors included in the BASFOR model:

$$CSE_{5-yr} \text{ (no thinning)} = {NEP_{5-yr}}\big/{GPP_{5-yr}} \qquad (1)$$

$$CSE_{lifetime} = {NECB_{lifetime}}\big/{GPP_{lifetime}} \qquad (2)$$

$$\text{with} \quad NECB = \frac{d(CLBS+CR+CSOM+CLITT)}{dt} \qquad (3)$$

$$NECB_{5-yr} \text{ (no thinning)} = NEP_{5-yr} \qquad (4)$$

$$NECB_{lifetime} = NEP_{lifetime} - CEXP_{thinning} \qquad (5)$$

The modelled CSE_{5-yr} can be contrasted with observation based CSE_{obs} (= NEP_{obs} / GPP_{obs}) derived from flux tower data over a similar, relatively short time period compared with a forest rotation (see Flechard et al., 2019). By extension, the $CSE_{lifetime}$ indicator quantifies the efficiency of C sequestration processes by a managed forest system, reflecting not only biological and ecophysiological mechanisms, but also the long term impact of human management through thinning frequency and severity.

For the N budget we define, by analogy to CSE, the N use efficiency (NUE) as the ratio of N immobilized in the forest system to the available mineral N, i.e. the ratio of tree N uptake (N_{upt}) to the total N_{supply} from internal SOM mineralization and N cycling processes (N_{miner}) and from external sources such as atmospheric N deposition (N_{dep}):

$$NUE = {N_{upt}}\big/{N_{supply}} \qquad\qquad (6)$$

with $\qquad N_{supply} = N_{miner} + N_{dep} \qquad\qquad\qquad\qquad\qquad (7)$

$\qquad\qquad\quad N_{supply} \approx N_{upt} + N_{leach} + N_{emission} \qquad\qquad\qquad (8)$

The fraction of N_{supply} not taken up in biomass and lost to the environment (N_{loss}) comprises dissolved inorganic N leaching
270 (N_{leach}) and gaseous NO and N_2O emissions ($N_{emission}$):

$$N_{loss} = {(N_{leach} + N_{emission})}\big/{N_{supply}} \qquad\qquad (9)$$

Note that i) NUE is *not* defined here as the amount of biomass produced per unit of N taken up from the soil, another
commonly used N use efficiency indicator, which would be NPP/N_{upt} (e.g. Finzi et al., 2007), and ii) biological N_2 fixation, as
well as N loss by total denitrification, are not accounted for in the current BASFOR version; also, leaching of dissolved
275 organic N and C (DON, DOC) and dissolved inorganic C (DIC) is not included either, all of which potentially impact budget
calculations.

2.2.4 Meta-modelling as a tool to standardize EC-based productivity data

One purpose of BASFOR modelling in this study was to gain knowledge on patterns of C and N fluxes, pools and internal
cycling that were not, or could not be, evaluated solely on the basis of the available measurements (for example, SOM
280 mineralization and soil N transfer; retranslocation processes at canopy level; patterns over the lifetime of a stand). The model
results were used to complement the flux tower observations to better constrain elemental budgets and assess potential and
limitations of C sequestration at the European forest sites considered here. Additionally, we used meta-modelling as an
alternative to multivariate statistics (e.g. stepwise multiple regression, mixed non-linear models, residual analysis) to isolate
the importance of N_r deposition from other drivers of productivity. This follows from the observations by Flechard et al.
285 (2019) that i) N_r deposition and climate were not independent in the dataset, and that ii) due to the large diversity of sites, the
limited size of the dataset, and incomplete information on other important drivers (e.g. stand age, soil type, management),
regression analyses were unable to untangle these climatic and other inter-relationships from the influence of N_r deposition.
BASFOR (or any other mechanistic model) is useful in this context, not so much to predict absolute fluxes and stocks, but to
investigate the relative importance of drivers, which is done by assessing changes in simulated quantities when model inputs
290 are modified. Meta-modeling involves building and using surrogate models that can approximate results from more
complicated simulation models; in this case we derived simplified relationships linking forest productivity to the impact of
major drivers, which were then used to harmonize observations from different sites. For example, running BASFOR for a
given site using meteorological input data from another site, or indeed from all other sites of the network, provides insight
into the impact of climate on GPP or NEP, all other factors (soil, vegetation structure and age, N_r deposition) being equal.
295 Within the boundaries of the network of 22 selected sites, this sensitivity analysis provides *relative* information as to which of
the 22 meteorological datasets is most, or least, favourable to growth for this particular site. This can be repeated for all sites
(22*22 climate «scenario» simulations). It can also be done for soil physical properties that affect the soil water holding
capacity (texture, porosity, rooting depth), in which case the result is a *relative* ranking within the network of the different
soils for their capacity to sustain an adequate water supply for tree growth. The procedure for the normalization of data
300 between sites is described hereafter.

Additional nitrogen affects C uptake primarily through releasing N limitations at the leaf level for photosynthesis (Wortman
et al., 2012; Fleischer et al., 2013), which scales up to GPP at the ecosystem level. Other major factors affecting carbon
uptake are related to climate (photosynthetically active radiation, temperature, precipitation), soil (for example water holding
capacity) or growth stage (tree age). In the following section, we postulate that observation-based gross primary productivity
305 (GPP_{obs}), which represents an actuation of all limitations in the real world, can be transformed through meta-modelling into a

standardized potential value (GPP*) for a given set of environmental conditions (climate, soil, age), common to all sites, thereby enabling comparisons between sites. We define GPP* as GPP_{obs} being modulated by one or several dimensionless factors (f_X):

$$GPP^* = GPP_{obs} \times f_{CLIM} \times f_{SOIL} \times f_{AGE} \qquad (10)$$

310   where the standardization factors f_{CLIM}, f_{SOIL} and f_{AGE} are derived from BASFOR model simulations corresponding to the CEIP/NEU time interval around 2005–2010, as described below. The factors involved in Eq. (10) address commonly considered drivers, but not nitrogen, which is later assessed on the basis of GPP*, rather than GPP_{obs}. Other potentially important limitations such as non-N nutrients, soil fertility, air pollution (O₃), poor ecosystem health, soil acidification, etc., are not treated in BASFOR, and cannot be quantified here. Further, the broad patterns of the GPP *vs.* N_{dep} relationships

315   reported in Flechard et al. (2019) did not show any marked difference between the three forest PFT (deciduous, pine, spruce), possibly because the datasets were not large enough and fairly heterogeneous. Thus, although PFT may be expected to influence C/N interactions, we did not seek to standardize GPP with an additional f_{PFT} factor.

   To determine the f_{CLIM} and f_{SOIL} factors, the model was run multiple times with all climate and soil scenarios for the n (=22) sites, a scenario being defined as using model input data or parameters from another site. Specifically, for f_{CLIM}, the model

320   weather inputs at each site were substituted in turn by the climate data (daily air temperature, global radiation, rainfall, wind speed and relative humidity) from all other sites; and for f_{SOIL}, the field capacity and wilting point parameters (Φ_{FC}, Φ_{WP}) and soil depth that determine the soil water holding capacity at each site (SWHC = (Φ_{FC} - Φ_{WP}) x soil depth), were substituted in turn by parameters from all other sites. Values of f_{CLIM} and f_{SOIL} were calculated for each site in several steps, starting with the calculation of the ratios of modelled GPP from the scenarios to the baseline value GPP_{base} such that:

325
$$X(i,j) = GPP(i,j)/GPP_{base}(i) \qquad (11)$$

where i (1..n) denotes the site being modelled and j (1..n) denotes the climate data set (j_{CLIM}) or soil parameter set (j_{SOIL}) used in the scenario being simulated (see Table S2 for the calculation matrices). The value of the X (i, j) ratio indicates whether the jth scenario is more (> 1) or less (< 1) favourable to GPP for the ith forest site.

   For each site, the aim of the f_{CLIM} factor (and similar reasoning for f_{SOIL}) (Eq. (10)) is to quantify the extent to which GPP

330   differs from a standard GPP* value that would occur if all sites were placed under the same climatic conditions. Rather than choose the climate of one particular site to normalize to, which could bias the analysis, we normalise GPP to the equivalent of a «mean» climate, by averaging BASFOR results over all (22) climate scenarios (Eq. (14)–(15)). However, since each of the scenarios has a different mean impact across all sites ($\overline{X(j)}$, Eq. (12)), we first normalize X(i,j) to $\overline{X(j)}$ value within each jth scenario (Eq. (13)):

335
$$\overline{X(j)} = {}^1\!/_n \sum_{i=1}^n X(i,j) \qquad (12)$$

$$X_{norm}(i,j) = X(i,j) \Big/ \overline{X(j)} \qquad (13)$$

The normalization of X (i, j) to X_{norm} (i, j) ensures that the relative impacts of each scenario on all n sites can be compared between scenarios. The final step is the averaging for each site of X_{norm} (i, j) values from all scenarios (either j_{CLIM} or j_{SOIL}) into the overall f_{CLIM} or f_{SOIL} values:

340
$$f_{CLIM}(i) = \overline{X_{norm}(i)} = {}^1\!/_n \sum_{j_{CLIM}=1}^n X_{norm}(i,j_{CLIM}) \qquad (14)$$

or
$$f_{SOIL}(i) = \overline{X_{norm}(i)} = {}^1\!/_n \sum_{j_{SOIL}=1}^n X_{norm}(i,j_{SOIL}) \qquad (15)$$

The factors f_{AGE} were determined by first normalizing modelled GPP (base run) to the value predicted at age 80, for every year of the simulated GPP time series at those m (=12) mature sites where stand age exceeded 80. The age of 80 was chosen since this was the mean stand age of the whole network. The following ratios were thus calculated:

345
$$Y(k,yr) = GPP_{base}(k,yr)/GPP_{base}(k,80) \qquad (16)$$

where k (1..*m*) denotes the mature forest site being modelled. A mean temporal curve for f_{AGE} (normalized to 80 years) was calculated, to be used subsequently for all sites, after the following:

$$f_{AGE}(yr) = \left(\frac{1}{m} \sum_{k=1}^{m} Y(k, yr) \right)^{-1} \tag{17}$$

3 Results

3.1 Short term (5-yr) versus lifetime C and N budgets from ecosystem modelling

Modelled C and N budgets are represented schematically in Fig. 1 and Fig. 2, respectively, as «Sankey» diagrams (Matlab «*drawSankey.m*» function; Spelling, 2009) for three example forest sites (DB5, EN3, EN16), and in Fig. S1–S6 of the Supplement for all sites of the study. Each diagram represents the input, output and internal flows in the ecosystem, with arrow width within each diagram being proportional to flow. For carbon (Fig. 1 and S1–S3), the largest (horizontal) arrows indicate exchange fluxes with the atmosphere (GPP, R_{eco}), while the smaller (vertical) arrows indicate gains (green) or losses (red) in internal ecosystem C pools (CSOM, CBS, CR, CL, CLITT), as well as any exported wood products (CEXP, orange). NEP is the balance of the two horizontal arrows, as well as the balance of all vertical arrows.

In the 5-yr simulations with no thinning occurring (Fig. 1-left; Fig. S1), NEP is equal to NECB, which is the sum of ecosystem C pool changes over time (= C sequestration if positive). By contrast, in the lifetime (since planting) simulations (Fig. 1-center; Fig. S2), the long-term impact of thinning is shown by the additional orange lateral arrow for C exported as woody biomass (CEXP). In this case, C sequestration or NECB no longer equals NEP, the difference being CEXP, the C contained in exported stems from thinned trees. By contrast, in the model, upon thinning the C from leaves, branches and roots join the litter layers or soil pools and is ultimately respired or sequestered. To compare between sites with different productivity levels, the lifetime data are also normalized as a percentage of GPP (Fig. 1-right; Fig. S3). The clear differences between 5-yr and lifetime C-budget simulations were: i) systematically larger GPP in recent 5-yr horizon (combined effects of age as well as CO_2 and N_{dep} changes over time); ii) C storage in branches and stems (CBS) dominated in both cases, but CBS fractions were larger in the 5-yr horizon; iii) larger relative storage in soil organic matter (CSOM) when calculated over lifetime.

For clarity in the N budgets (Fig. 2 and S4–S6), the largest (horizontal) arrows indicate the modelled internal ecosystem N cycling terms (N_{miner} from SOM mineralisation, N_{upt} uptake by trees) and the secondary (vertical) arrows represent external exchange (inputs and losses) fluxes as N_{dep}, N_{leach} and $N_{emission}$ (unit: g (N) m^{-2} yr^{-1}). The variable NMIN describes the transient soil inorganic N pool in the soil solution and adsorbed on the soil matrix (NMIN = NO_3^- + NH_4^+; units g (N) m^{-2}). Since there is no significant long term (multi-annual) change in NMIN, the total mineral N_{supply} (defined as $N_{miner} + N_{dep}$) is basically balanced by N uptake (N_{upt}) and losses ($N_{leach} + N_{emission}$) (Eq. (8)). Modelled N budgets were calculated for a 5-yr time horizon (Fig. 2-left; Fig. S4) and for the whole time period since the forest was established (lifetime, Fig. 2-center; Fig. S5). Lifetime data were also normalized as a percentage of N_{supply} (Fig. 2-right; Fig. S6). The clear differences between 5-yr and lifetime N-budget simulations are: i) N_{loss} and especially N_{leach} were significantly larger over the stand lifetime since planting; ii) N_{upt} was a larger fraction of total N_{supply} over the recent 5-yr period.

{Insert Fig. 1 here}

{Insert Fig. 2 here}

3.2 Contrasted carbon and nitrogen use efficiencies

Collectively, the changes in the ecosystem C pools, especially the increases in stems and branches (CBS), roots (CR) and soil organic matter (CSOM) represent roughly 20–30% of GPP for both 5-yr and lifetime simulations (Fig. 1, S1–S3). By contrast, the analogous term for the N, the N_{upt} fraction of total N_{supply}, is a much more variable term, both between sites of the network and between the 5-yr and lifetime simulations (Fig. 2, S4–S6). Modelled lifetime CSE and NUE values are

compared in Fig. 3 with the 5-yr values, as a function of stand age, indicating that (i) the more mature forests of the network (age range ~80–190 yrs) tend to have larger NUE than younger forests (~30–60 yrs), and (ii) the difference in NUE between young *vs.* mature forests is especially clear if NUE is calculated over the whole period since planting (lifetime). These observations are plausible and consistent with current understanding of long term N cycling in planted forests, incorporated in

390   the model structure, equations and parameters. Namely, (i) is a consequence of BASFOR predicting larger relative N_{loss} in younger stands, in which lower N demand by a smaller living biomass, combined in the early years with enhanced N_{miner} from higher soil temperature (canopy not yet closed) and with a larger drainage rate (smaller canopy interception of incident rainfall), all lead to larger NMIN losses. Observation (ii) is a mathematical consequence of high N losses during the forest's early years having a larger impact on lifetime calculations in younger than mature forests. NUE tends to reach 70-80% on

395   average after 100 years and is smaller calculated from lifetime than from a 5-yr thinning-free period. For forests younger than 60 years, lifetime NUE is only 60%; the 5-yr thinning-free value can be larger, but thinning events are likely to be more frequent at that age.

Modelled carbon sequestration efficiency is less affected than NUE by forest age (CSE range ~15–30%) (Fig. 3). There is a tendency for 5-yr (thinning-free) CSE to decrease from ~30% to ~20% between the ages of 30 and 190 years. This means

400   that, in the model, R_{eco} in 30 to 60-yr old stands represents a smaller fraction of GPP than in mature stands, which is a consequence of i) R_{aut} being a constant fraction of GPP in the model, ii) R_{het} being a linear function of fast and slow C pools in litter layers and SOM, and iii) soil and litter layers C pools evolving non-linearly with GPP as the forest grows older. Lifetime CSE values are slightly smaller than 5-yr values: the difference corresponds to cumulative CEXP over time, but the trend with age is weaker than for 5-yr CSE. The relatively narrow range of modelled 5-yr CSE values (20–30%) is in sharp

405   contrast to the much wider range of observation-based CSE_{obs} values (from -9% to 61%), likely reflecting some limitations of the model and possibly also measurement uncertainties, as discussed in Flechard et al. (2019).

{Insert Fig. 3 here}

Beyond the overall capacity of the forest to retain assimilated C (as quantified by CSE), the modelled fate of sequestered C, the simulated ultimate destination of the C sink, is also a function of forest age and of the time horizon considered (Fig. 4).

410   The fraction of NECB sequestered in above-ground biomass (CLBS) over a recent 5-yr horizon is on average around 80% (*versus* around 10% each for CR and CSOM) and not clearly linked to forest age, i.e. the model does not simulate any slowing down with age of the annual growth of above-ground biomass. Calculated over lifetimes, the dominant ultimate destination of sequestered C remains CLBS. However, this fraction is smaller (50–60%) in old-growth forests than in younger stands (60–80%), since a larger cumulative fraction of above-ground biomass (timber) will have been removed

415   (CEXP) by a lifetime of thinnings in a mature forest, while the cumulative gain in CSOM is not repeatedly depleted, but on the contrary enhanced, by thinnings (since the model assumes bole removal only, not total tree harvest). Modelled annual C storage to the rooting system clearly declines with age and is an increasingly marginal term over time (although the absolute CR stock itself keeps increasing over time, except when thinning transfers C from roots to SOM).

{Insert Fig. 4 here}

420   **3.3 Standardization of observation-based GPP through meta-modelling**

The purpose of meta-modelling was to standardize observation-based GPP_{obs} into GPP* through model-derived factors that separate out the effects of climate, soil and age between monitoring sites (Eq. (10)), so that the importance of N_r can be isolated. The sensitivity of modelled GPP to climate and soil physical properties was tested through various model input and parameter scenarios, allowing standardization factors f_{CLIM} and f_{SOIL} to be calculated as described in Methods (Eq. (11)–(15))

425   and Table S2 in the Supplement. The resulting distributions of all simulations for all sites were represented in Fig. 5 as «violin» plots (Matlab «*distributionPlot*.m» function; Dorn, 2008) for the climate-only and soil-only scenarios (n^2 = 484 simulations each), and also combined climate*soil scenarios (n^3 = 10648 simulations). For each site, the scenarios explore the modelled response of ecosystem C dynamics to a range of climate and soil forcings different from their own. The size and

430 position of the violin distribution indicate, respectively, the degrees of sensitivity to- and limitation by- climate, soil, or both; a site is especially limited by either factor (relative to the other sites of the network) when the baseline/default run (GPP$_{base}$) is located in the lower part of the distribution.

Similarly, to account for the effect of tree age, the f$_{AGE}$ factor was calculated following Eq. (17), whereby the time series for the ratio of modelled GPP$_{base}$(yr) to GPP$_{base}$(80) (Eq. (16)) followed broadly similar patterns for the different sites (Fig. 6), with values mostly in the range 0.6–0.8 at around age 40, crossing unity at 80 and levelling off around 1.2–1.4 after a century.

435 Some of the older sites (e.g. EN2, EN6, EN15) showed a peak followed by a slight decrease in modelled GPP, but not at the same age. This was due to a peak in N$_{dep}$ in the early 1980's in Europe (see Fig. S4 in the Supplement to Flechard et al., 2019), with the N$_{dep}$ peak occurring at different ontogenetic stages in the differently aged stands. By calculating a mean f$_{AGE}$ factor across sites the peak N$_{dep}$ effect was smoothed out (Fig. 6). Thus, for a younger forest, the multiplication of GPP$_{obs}$ by f$_{AGE}$ (>1) simulated the larger GPP* that one could expect for the same site at 80 yr; conversely, the GPP* a mature forest

440 (>100 yr) would be reduced compared with GPP$_{obs}$.

{Insert Fig. 5 here}

{Insert Fig. 6 here}

The combined modelled effects of climate, soil, and stand age on GPP are summarized in Fig. 7. Values for both f$_{CLIM}$ and f$_{SOIL}$ are mostly in the range 0.7–1.5, and are predictably negatively correlated to mean annual temperature (MAT) and soil

445 water holding capacity (SWHC), respectively (Fig. 7A). A value well above 1 implies that GPP$_{obs}$ for one site lies below the value one might have observed if climate or SWHC had been similar to the average of all other sites of the network. In other words this particular site was significantly limited by climate, SWHC, or both, relative to the other sites. Conversely, a value below 1 means that GPP at the site was particularly favoured by weather and soil. Climate or soil conditions at some sites have therefore the potential to restrict GPP by around one third, while other climates or soil conditions may enhance GPP by

450 around one third, compared with the average conditions of the whole network. Applying the f$_{CLIM}$, f$_{SOIL}$ and f$_{AGE}$ multipliers to GPP$_{obs}$ (Eq. (10)) provides a level playing field (GPP*) for later comparing sites with respect to N$_r$ deposition, but also increases the scatter and noise in the relationship of GPP* to N$_{dep}$, particularly with the introduction of f$_{AGE}$ (Fig. 7B).

{Insert Fig. 7 here}

3.4 Response of gross primary productivity to N$_r$ deposition

455 The standardized forest GPP* values, i.e. GPP*(f$_{CLIM}$), GPP*(f$_{CLIM}$ x f$_{SOIL}$) and GPP*(f$_{CLIM}$ x f$_{SOIL}$ x f$_{AGE}$), show in the N$_{dep}$ range 0–1 g (N) m^{-2} yr^{-1} a much less steep relationship to N$_{dep}$ than the original GPP$_{obs}$ (Fig. 7B). This supports the hypothesis that GPP at low N$_{dep}$ sites is also limited by climate and/or soil water availability. In Fig. 7B, 2nd-order polynomials are fitted to the data to reflect the strong non-linearity present in GPP$_{obs}$, driven especially by the 4 highest N$_{dep}$ sites (>2.5 g (N) m^{-2} yr^{-1} at EN2, EN8, EN15 and EN16). The non-linearity (magnitude of the 2nd-order coefficient) is reduced

460 by the introduction of f$_{CLIM}$ and f$_{SOIL}$, while f$_{AGE}$ has a small residual impact on the shape of the regression. Due to this non-linear behaviour, the dGPP/dN$_{dep}$ responses decrease with N$_{dep}$ for the observation-based GPP, but less so for the standardized GPP* estimates (Fig. 7C). Values of dGPP$_{obs}$/dN$_{dep}$ (calculated for each N$_{dep}$ level by the slope of the tangent line to the quadratic fits of Fig. 7B) range from around 800 g (C) g^{-1} (N) at the lowest N$_{dep}$ level down to negative values at the highest N$_{dep}$ sites; for the standardized GPP* accounting for all climate, soil and age effects, this range is much narrower, from

465 around 350 down to near 0 g (C) g^{-1} (N).

Average dGPP/dN$_{dep}$ figures that are representative of this set of forest sites are given in the upper part of Table 2, either calculated over the whole range of 22 sites, or for a subset of 18 sites that excludes the four highest deposition sites (>2.5 g (N) m^{-2} yr^{-1}). If all modelled sites are considered, the mean dGPP/dN$_{dep}$ regression slopes are smaller (190–260 g (C) g^{-1} (N)), being influenced by the reductions in GPP at very high N$_{dep}$ levels, possibly induced by the negative side effects of N

470 saturation. If these four sites are excluded, the mean dGPP/dN$_{dep}$ is larger (234–425 g (C) g^{-1} (N)), reflecting the fact that healthier, N-limited forests are more responsive to N additions. In this subset of 18 sites, the effects of climate, soil and stand

age account for approximately half of GPP (the mean $dGPP/dN_{dep}$ response changes from 425 to 234 g (C) g^{-1} (N)). For comparison, Table 2 also provides the values of $dGPP_{obs}/dN_{dep}$ obtained directly through simple linear regression for all forest sites and for the semi-natural vegetation sites, with values of the same order (432 and 504 g (C) g^{-1} (N), respectively) if the

475 high N deposition sites ($N_{dep} > 2.5$ g (N) m^{-2} yr^{-1}) are removed.

As a further comparison, an additional BASFOR modelling experiment is shown in Fig. 8A, in which GPP at all sites is simulated in a range of N_{dep} scenarios (0, 0.1, 0.2, 0.5, 1, 1.5, 2, 2.5, 3, 3.5, 4 and 4.5 g (N) m^{-2} yr^{-1}, constant over lifetime) to substitute for the actual N_{dep} levels of each site. Around half the sites show a steadily increasing (modelled) GPP as N_{dep} increases over the whole range 0–4.5 g (N) m^{-2} yr^{-1}, with broadly similar slopes between sites; while the other half levels off

480 and reaches a plateau at various N_{dep} thresholds, indicating that beyond a certain level N_{dep} is no longer limiting, according to the model. For comparison with the dC/dN responses calculated previously for GPP$_{obs}$ and GPP* in Fig. 7B-C and Table 2, we derive a mean modelled $dGPP/dN_{dep}$ response from a linear regression of Fig. 8A data over the range 0–2.5 g (N) m^{-2} yr^{-1} (i.e. excluding the highest deposition levels). This yields a mean $dGPP/dN_{dep}$ slope across all sites of 297 (273–322) g (C) g^{-1} (N) for the N_{dep} model experiment, only marginally larger than the three GPP* average slopes of Table 2. Note that in Fig.

485 7B, the response of GPP* to N_{dep} is calculated *between sites* of the network, while in Fig. 8A the GPP to N_{dep} response is calculated *within each site* from the model scenarios, then averaged across all sites.

{Insert Fig. 8 here}

3.5 Response of net ecosystem productivity to N_r deposition

Similarly to GPP, the NEP and NECB responses to N_{dep} cannot be reliably inferred directly from EC-flux network data given

490 the large variability between sites in climate, soil type, age and other constraints to photosynthesis and ecosystem respiration. However, plausible estimates can be obtained by applying a range of mean CSE indicators (as defined previously) to project the normalized GPP* responses to N_{dep} (Table 2). Carbon sequestration efficiencies for forests are confined to a narrow range (17–31% of GPP, average μ=22%, standard deviation σ=4%) in model simulations over 5-yr (no thinning) time horizons (Fig. 3); they vary considerably more in EC-based observations (range -9 to 61%, σ=17%), but with a similar mean (μ=25%).

495 CSE metrics express the GPP fraction not being respired (R$_{eco}$) or exported (C$_{EXP}$) out of the ecosystem. Multiplied by the $dGPP/dN_{dep}$ slope they provide estimates of the net ecosystem C gain per unit N deposited (Table 2).

Short-term (5-yr) mean estimates for NEP responses, based on average CSE from both observations (CSE$_{obs}$) and modelling (CSE$_{5-yr}$), and accounting for GPP climate/soil/age normalization, range from 41 to 47 g (C) g^{-1} (N), averaged over all sites, or 51 to 57 g (C) g^{-1} (N) removing the four highest N_{dep} sites (middle part of Table 2). Predictably, lifetime estimates for

500 $dNECB/dN_{dep}$ responses are about 20% smaller, on the order of 34–42 g (C) g^{-1} (N). For comparison, the mean 5-yr $dNEP/dN_{dep}$ obtained directly by BASFOR modelling of N_{dep} scenarios for all sites (Fig. 8B) was larger (76 ± 7 g (C) g^{-1} (N)) than the measurement-based, model-corrected estimates of Table 2.

If the forest NEP response to N_{dep} is calculated directly through simple linear or quadratic regression of NEP$_{obs}$ *vs.* N_{dep} (bottom part of Table 2), therefore not including any standardization of the data, the dC/dN slope is much larger (178–224 g

505 (C) g^{-1} (N)) within the N_{dep} range 0–2.5 g (N) m^{-2} yr^{-1}. If all forest sites are considered (including N-saturated sites with N_{dep} up to 4.3 g (N) m^{-2} yr^{-1}), the dC/dN slope is much smaller (71–108 g (C) g^{-1} (N)), but this only reflects the reduced NEP observed at those elevated N_{dep} sites (see Fig. 4C in Flechard et al., 2019), with altogether very large scatter and very small R^2. Equivalent figures for (not standardized) semi-natural NEP *vs.* N_{dep} appear to be significantly smaller (34–89 g (C) g^{-1} (N)) than in forests.

510 If the meta-modelling standardization procedure for climate, soil and age is attempted (for comparison only) directly on NEP, as opposed to the preferred procedure using GPP (Eq. (10)–(17)), the simulated f$_{CLIM}$, f$_{SOIL}$ and f$_{AGE}$ reduce the NEP response to N_{dep} by only 18%, from 178 down to 146 g (C) g^{-1} (N) (bottom part of Table 2), while the equivalent reduction for GPP was 45%. The resulting figure (112–146 g (C) g^{-1} (N)) is likely much over-estimated, around factor of 2–3 larger than those

obtained through the stepwise method using CSE * $dGPP/dN_{dep}$. Standardization factors derived from BASFOR meta-
modelling are more reliable for GPP than for NEP, since model performance is significantly better for GPP than for R_{eco} and
hence NEP (Fig. 6 in Flechard et al., 2019).

{Insert Table 2 here}

4 Discussion

4.1 A moderate non-linear response of forest productivity to N_r deposition

The C sequestration response to N_{dep} in European forests was derived using a combination of flux tower-based C and N
exchange data and process-based modelling, while a number of previous studies have been based on forest inventory methods
and stem growth rates (e.g. de Vries et al.2009; Etzold et al., 2014). The main differences with previous meta-analyses that
were also based on EC-flux datasets (e.g. Magnani et al., 2007; Fleischer et al., 2013; Fernández-Martínez et al., 2014, 2017),
were that i) we derived total N_{dep} from local measurements of the wet and dry fractions as opposed to regional/global CTM
outputs; ii) we untangled the N_{dep} effect from climatic, soil and other influences by means of a mechanistic model, not
through statistical methods; and iii) in Flechard et al. (2019) we estimated ecosystem-level N, C and GHG budgets calculated
through a combination of local measurements, mechanistic and empirical models, and database and literature data mining.

Our most plausible estimates of the dC/dN response of net productivity over the lifetime of a forest are of the order of 40–50
g (C) g^{-1} (N) on average over the network of sites included in the study (Table 2). Such values are broadly in line with the
recent reviews by Erisman et al. (2011) and by Butterbach-Bahl et al. (2011) (range 35–65 g (C) g^{-1} (N)), but slightly larger
than estimates given in a number of other studies (e.g. Liu and Greaver, 2009; de Vries et al., 2009, 2014). Given the
considerable uncertainty attached to these numbers (Table 2), they cannot be considered significantly different from any of
those earlier studies. The meta-modelling-based approach we describe for normalizing forest productivity data to account for
differences in climate, soil and age among sites, reduces the net productivity response to N_{dep} by roughly 50%, which is of the
same order as the results (factor of 2–3 reduction) of a similar climate normalization exercise by Sutton et al. (2008). This
means that not accounting for inter-site differences would have led to an over-estimation of the dC/dN slope by a factor of 2.
Observations and model simulations both indicate that the N_{loss} fraction of N_{supply} increases with N_{dep}; thus, at many sites but
especially those with $N_{dep} > 1.5–2$ g (N) m^{-2} yr^{-1}, N availability is not limiting forest growth. In such cases it becomes
meaningless to try to quantify a N fertilisation effect. Indeed, despite large uncertainties in measured data and in model-
derived normalization factors, the non-linear trend is robust, with dC/dN values tending to zero in N-saturated forests (>2.5–3
g (N) m^{-2} yr^{-1}). In their review paper De Vries et al. (2014) gave a range of N_{dep} levels varying between 1.5–3 g (N) m^{-2} yr^{-1}
beyond which growth and C sequestration were not further increased or even reversed. These findings suggest that in areas of
the world where N_{dep} levels are larger than 2.5–3 g (N) m^{-2} yr^{-1}, which now occur increasingly in Asia, specifically in parts of
China, Japan, Indonesia, and India (Schwede et al., 2018), the forecast increased N_r emissions and increased N_{dep} levels may
thus not have a positive impact on the continent's land based CO_2 sink. Data treatment and selection in our dataset (e.g.
removal of N-saturated forests) strongly impacted the plausible range of dC/dN responses (Table 2) derived from the original
data. The non-linearity of ecosystem productivity relationships to N_{dep} (Butterbach-Bahl and Gundersen, 2011; Etzold et al.,
2014) limits the usefulness and significance of simple linear approaches. These data suggest that there is no single dC/dN
figure applicable to all ecosystems, that the highly non-linear response depends on current and historical N_{dep} exposure levels,
and on the degree of N saturation, although other factors than N, discussed later, may also be involved.

For the short semi-natural vegetation sites, included in the study as a non-fertilised, non-woody contrast to forests, the
apparent impact of N_{dep} on GPP_{obs} was of the same order as in forests, but likely much smaller than in forests when
considering NEP_{obs} (Table 2). This is in principle consistent with the hypothesis (de Vries et al., 2009) that the ecosystem
dC/dN response may be larger in forests due to the large C/N ratio (200–500) of above-ground biomass (stems and branches),

555 where much of the C storage occurs (up to 60–80% according to BASFOR, Fig. 4); whereas in semi-natural ecosystems C storage in SOM dominates, with a much lower C/N ratio (10–40). However, this comparison of semi-natural *versus* forests is based on NEP$_{obs}$ that was not normalized for inter-site climatic and edaphic differences, since no single model was available to carry out a meta-modelling standardization for all the different semi-natural ecosystem types (peatland, moorland, fen, grassland), and therefore these values must be regarded as highly uncertain.

560 **4.2 Limitations and uncertainties in the approach for quantifying the dC/dN response**

Monitoring atmospheric gas-phase and aerosol N$_r$ contributed to reducing the large uncertainty in total N$_r$ deposition at individual sites, because dry deposition dominates over wet deposition in most forests (Flechard et al., 2019), except at sites a long way from sources of atmospheric pollution, and because the uncertainty in dry deposition and its modelling is much larger (Flechard et al., 2011; Simpson et al., 2014). However, despite the considerable effort involved in coordinating the

565 continental-scale measurement network (Tang et al., 2009), the number of forest sites in this study (31) was relatively small compared with other studies based on ICP (de Vries et al., 2009; ICP, 2019) or other forest growth databases, or global-scale FLUXNET data (hundreds of sites worldwide; see Burba, 2019). Thus, the gain in precision of N$_{dep}$ estimates from local measurements was offset by the smaller population sample size. Nonetheless this study does show the added value of the N$_r$ concentration monitoring exercise and the need to repeat and extend such initiatives.

570 Understanding, quantifying and reducing all uncertainties leading up to dC/dN estimates are key issues to explore. Apart from measurement uncertainties in N$_r$ deposition and losses, and in the C balance based on EC measurements, analysed in the companion paper, the major difficulties that arose when assessing the response to N$_{dep}$ of forest productivity included:

i)   The heterogeneity of the population of forests, climates and soils in the network, and the large number of potential drivers relative to the limited number of sites, hindered the use of a straightforward, regression-based

575   analysis of observational data without a preliminary (model-based) harmonization;

ii)   The model-based normalization procedure for GPP, used to factor out differences in climate, soil and age among sites, significantly amplified the noise in C/N relationships, an indication that the generalized modelled effects may not apply to all individual sites and that other important ecological determinants affecting forest productivity are missing in the BASFOR model;

580 iii) The EC measurement-based ratio of R$_{eco}$ to GPP (=1-CSE) was very variable among forests and this high variability cannot be explained or simulated by the ecosystem model we used, i.e. more complex model parameterizations of R$_{aut}$ and R$_{het}$ may be required to better represent the diversity of situations and processes;

iv)   Nitrogen deposition likely contributes a minor fraction (on average 20% according to the model) of total ecosystem N supply (heavily dominated by soil organic N mineralization), except for the very high deposition

585   sites (up to 40%). Thus, in many cases the N$_{dep}$ fertilisation effect may be marginal and difficult to detect, because it may be smaller than typical measurement uncertainties and noise in C and N budgets.

The EC-based flux data suggest that the N$_{dep}$ response of forest productivity is clearer at the gross photosynthesis level, in patterns of (normalized) GPP differences among sites, than at the NEP level, where very large differences in CSE among sites lead to a de-coupling of N$_{dep}$ and NEP. The response of GPP to N$_{dep}$ appeared to be reasonably well constrained by both EC

590 flux measurements and BASFOR modelling, which is why we chose to normalize GPP, not NEP. The significantly better model performance obtained for GPP than for R$_{eco}$ and NEP (Fig. 6 in Flechard et al., 2019) likely reveals a relatively poor understanding and mathematical representation of R$_{eco}$ (especially for the soil heterotrophic and autotrophic components)$_t$, and the factors controlling their variability among sites. The large unexplained variability in CSE and C sequestration potentials may also involve other limiting factors that could not be accounted for in our measurement/model analysis, since

595 they are not treated in BASFOR. Such factors may be related to soil fertility, ecosystem health, tree mortality, insect or wind damages in the previous decade, incorrect assumptions on historical forest thinning, all affecting general productivity patterns.

4.3 What drives the large variability in carbon sequestration efficiency?

Carbon sequestration efficiency metrics are directly and negatively related to the ratio of R_{eco} to GPP, expressing the
600   likelihood that one C atom fixed by photosynthesis will be sequestered in the ecosystem. Earlier FLUXNET-based statistical
meta-analyses have demonstrated that although R_{eco} is strongly dependent on temperature on synoptic or seasonal scales
(Mahecha et al., 2010; Migliavacca et al., 2011), GPP is the key determinant of spatial variations in R_{eco} (Janssens et al.,
2001; Migliavacca et al., 2011; Chen et al., 2015), and further, that the fraction of GPP that is respired by the ecosystem is
highly variable (Fernández-Martínez et al., 2014), and more variable than in current model representations. We have used
605   three different CSE indicators, averaged across all sites, to derive a NEP/N_{dep} response from model-standardized GPP* data
(Table 2). Values of CSE_{obs} varied over a large range among sites (-9 to 61%, Fig. 9). Some of the variability might be due to
measurement errors, but small (<10%) or large (>40%) CSE_{obs} values could also genuinely reflect the influence or the
absence of ecological limitations related to nutrient availability or vegetation health.

4.3.1 From nutrient limitation to nitrogen saturation

610   Can nutrient limitation (nitrogen or otherwise) impact ecosystem carbon sequestration efficiency? Soil fertility has been
suggested to be a strong driver at least of the forest biomass production efficiency (BPE), defined by Vicca et al. (2012) as
the ratio of biomass production to GPP, with BPE increasing in their global dataset of 49 forests from 42% to 58% in soils
with low- to high-nutrient availability, respectively. The study by Fernández-Martínez et al. (2014) of 92 forest sites around
the globe reported a large variability in CSE (=NEP/GPP calculated from FLUXNET flux data), which they suggest is
615   strongly driven by ecosystem nutrient availability (ENA), with CSE levels below 10% in nutrient-poor forests and above 30%
in nutrient-rich forests. The range of CSE values derived from flux measurements in our study (CSE_{obs} in Table 2) was
similarly large, even though all of our sites were European and our dataset size was one third of theirs (N=31, of which 26
sites in common with Fernández-Martínez et al., 2014). We did not attempt in this study to characterize a general indicator of
ENA beyond total N_r deposition; but if we use the high, medium or low (H, M, L) scores of ENA attributed to each site
620   through factor analysis of nutrient indicators by Fernández-Martínez et al. (2014), we find that the H group (7 sites) has a
mean CSE_{obs} of 32% (range 16–48%), the M group is slightly higher (7 sites, mean 39%, range 21–61%), while the L group
has indeed a significantly smaller mean CSE_{obs} of 14% (12 sites, range -9 to 38 %). Interestingly, the mean N_{dep} levels for
each group are H = 1.5 (range 0.5–2.3) g (N) m^{-2} yr^{-1} , M = 2.1 (range 1.1–4.2) g (N) m^{-2} yr^{-1} and L = 1.3 (range 0.3–4.1) g
(N) m^{-2} yr^{-1}, i.e. the highest mean CSE_{obs} of the three groups is found in the group with the highest mean N_{dep} (M).

625   The nutrients and other indicators of fertility considered by Fernández-Martínez et al. (2014) included, in addition to N, P,
soil pH, C/N ratios and cation exchange capacity, as well as soil texture and soil type. However, very few sites were fully
documented (see their Supplement Table S1), data were often qualitative, and other key nutrients were not included in the
analysis (K, Mg and other cations; S also has been suggested to have become a limiting factor for forest growth following
emission reductions, see Fernández-Martínez et al., 2017). The extent to which the overall fertility indicator quantified by
630   ENA was driven by nitrogen in the Fernández-Martínez et al. (2014) factor analysis is not evident. At sites where other
nutrients are limiting, the response to N additions would be small or negligible regardless of whether N itself is limiting. This
places severe constraints on the interpretation of productivity data in response to N_{dep}, since most current models, which do
not account for other nutrient limitations, cannot be called upon to normalize for differences between sites.

The impact of the fertility classification on CSE of the sites included in Fernández-Martínez et al. (2014) was questioned by
635   Kutsch and Kolari (2015) on the basis of unequal quality of the EC-flux datasets found in FLUXNET and other databases. By
excluding complex terrain sites (and young forests) from the Fernández-Martínez et al. (2014) dataset, Kutsch and Kolari
(2015) calculated a much reduced variability in CSE, with a «reasonable» mean value of 15% (range 0–30%), and suggesting
a much lower influence of nutrient status than claimed by Fernández-Martínez et al. (2014). In their reply, Fernández-
Martínez et al. (2015) re-analyzed the same subset of sites selected by Kutsch and Kolari (2015), but using the same

640 generalized linear model as used in their original analysis of the whole dataset, as opposed to the linear model used by Kutsch
and Kolari (2015). Fernández-Martínez et al. (2015) then maintained that the findings of the original study were still valid for
the restricted dataset, i.e. that the nutrient status had a significant influence on CSE.

The smaller European dataset of our study poses a similar dilemma. The much wider variation in CSE_{obs} than modelled $CSE_{5\text{-}yr}$ may both point to possible measurement issues if CSE_{obs} values (especially the larger ones) are considered ecologically

645 implausible, and/or inform on important ecological processes that are not accounted for in the model. Among the forests in
our study that seemed particularly inefficient (CSE_{obs} <10%) at retaining photosynthesized carbon (EN4, EN6, EN8, EN11,
EN17, EB5), all were classified as L (low ENA) in Fernández-Martínez et al. (2014) and two (EN6, EN11) were even net C
sources (R_{eco} > GPP). The EN4, EN6, EN17 sites had the three largest soil organic contents (SOC, Fig. 9A), which may have
induced larger rates of heterotrophic respiration, but EN4 has also been reported as having unrealistically large ecosystem

650 respiration rates (Anthoni et al., 2004). The EN8 site (mature pine-dominated forest in Belgium) was very unlikely to be N-
or S-limited, having been under the high deposition footprint of Antwerp petrochemical harbour and local intensive
agriculture for decades, even if emissions have declined over the last 20 years (Neirynck et al., 2007, 2011). However, the
comparatively low LAI, GPP and CSE (Fig. 4 in Flechard et al., 2019) at this site are likely not independent of the historical,
N- and S-induced soil acidification, which has worsened the already low P and Mg availabilities (Janssens et al., 1999), and

655 from which the forest is only slowly recovering (Neirynck et al., 2002; Holmberg et al., 2018). This site is actually an
excellent example to illustrate the complex web of biogeochemical and ecological interactions, which further complicate the
quantification of the (single-factor) N_{dep} impact on C fluxes. By not accounting for the low Mg and P availabilities and the
poor ecosystem health, the BASFOR model massively over-estimated GPP, R_{eco} and NEP at EN8 (Fig. 6 in Flechard et al.,
2019). In fact, based on prior knowledge of this site's acidification history, and since such mechanisms and impacts are not

660 mathematically represented in BASFOR, EN8 was from the start discarded from the calibration dataset for the Bayesian
procedure (Cameron et al., 2018). The four lowest CSE_{obs} values were found at sites with topsoil pH < 4 (Fig. 9C), although
other forests growing on acidic soils had reasonably large CSE_{obs} ratios.

The large variability in CSE_{obs} cannot be explained by any single edaphic factor (Fig. 9A-C), more likely by a combination of
many factors that may include N_{dep} (Fig. 9E). As noted previously, C flux measurements at all four forest sites with N_{dep} > 2.5

665 g (N) m^{-2} yr^{-1} (EN2, EN8, EN15, EN16) indicated lower productivity estimates than those in the intermediate N_{dep} range, or at
least smaller than might have been expected from a linear N fertilisation effect (Fig. 4 in Flechard et al., 2019). EN2 (spruce
forest in southern Germany) is also well-documented as an N-saturated spruce forest with large total N losses (~3 g (N) m^{-2}
yr^{-1}) as NO, N_2O and NO_3^- (Kreutzer et al., 2009), but its productivity and CSE are not affected to the same extent as EN8.
Not all the difference is necessarily attributable to the deleterious impacts of excess N_r deposition, as suggested by the GPP

670 normalization exercise (Fig. 7). For example, EN15 and EN16, planted on sandy soils, appear from meta-modelling to suffer
from water stress comparatively more than the average of all sites (Fig. 5-Soil), if indicators of soil water retention based on
estimates of soil depth, field capacity and wilting point can be considered reliable.

4.3.2 Forest age

Forest age is expected to affect photosynthesis (GPP), growth (NPP), carbon sequestration (NEP) and CSE for many reasons.

675 A traditional view of the effect of stand age on forest NPP (Odum, 1969) postulated that R_{aut} increases with age and
eventually nearly balances a stabilized GPP, such that NPP approaches zero upon reaching a dynamic steady state. Revisiting
the paradigm, Tang et al. (2014) found that NPP did decrease with age (> 100 yr) in boreal and temperate forests, but the
reason was that both GPP and R_{aut} declined, with the reduction in forest growth being primarily driven by GPP, which
decreased more rapidly with age than R_{aut} after 100 years. However, the ratio NPP/GPP remained approximately constant

680 within each biome.

The effect of age on NEP and CSE is even more complex since this involves not only changing successional patterns of GPP
and R_{aut}, but also of R_{het} over a stand rotation of typically one century or more, which is much longer than the longest

available flux datasets. Therefore age effects are often studied by comparing differently aged forest sites across the world, which introduces many additional factors of variation, including differences in water availability, soil fertility, or even tree

685 species, genera, or PFTs. Forest and tree ages should in theory be normalized to account for species-specific ontogeny patterns, i.e. the age of 80 years may be relatively young for some species, and quite old for others, and therefore population dynamics may be very different for the same age. Nevertheless, forest age has been suggested to be a dominant factor controlling the spatial and temporal variability in forest NEP at the global scale, compared with abiotic factors such as climate, soil characteristics and nutrient availability (Besnard et al., 2018). In that study, the multivariate statistical model of

690 NEP, using data from 126 forest eddy-covariance flux sites worldwide, postulated a non-linear empirical relationship of NEP to age, adapted from Amiro et al. (2010), whereby NEP was negative (a net C source) for only a few years after forest establishment, then increased sharply above 0 (a net C sink), stabilized after around 30 years and remained at that level thereafter for mature forests (> 100 years). This model, therefore, did not assume any significant reduction in forest net productivity after maturiy, up to 300 years, consistent with several synthesis studies that have reported significant NEP of

695 centuries-old forest stands (Buchmann and Schulze, 1999; Kolari et al., 2004; Luyssaert et al., 2008).

By analogy, our approach for accounting for the age effect was based on the modelled time course of GPP (Eq. (16)-(17)), which in the BASFOR model tended to stabilize after 100 years, and subsequently using a mean CSE that did not depend on stand age. However, the variability in CSE_{obs} appeared to be much larger in mature forests (>80 years) than in the younger stands (Fig. 9D). For the younger forests (<60 years, all sites probably still in an aggrading phase), the CSE_{obs} values were in

700 a narrow band of 15–30% and were well represented by model simulations, with the exceptions of EN1, EB3 at around 50% and of EN4 being near 0% (all three locations being high elevation sites with complex terrain and potential EC measurement issues, see Flechard et al., 2019). By contrast, values for mature forests were either below 15% or above 30%. For some cold sites such as EN6 and EN11, growing in low nutrient environments (e.g. peat at EN6) with high SOC (Fig. 9A) and/or high soil C/N ratio (Fig. 9B) and low soil pH (Fig. 9C), or for the N-saturated and acidified EN8 site, the low CSE is not

705 necessarily linked to age. Aging, senescence and acidification may at some point curb sequestration efficiency in older forests, but even excluding the complex terrain sites, there remain a good number of productive mature sites with CSE_{obs} in the range 30–40%, which questions the Odum (1969) paradigm of declining net productivity and C equilibrium in old forests.

{Insert Fig. 9 here}

4.3.3 Does nitrogen deposition impact soil respiration?

710 The overall net effect of N_r deposition on carbon sequestration must include not only productivity gains, but also indirect, positive or negative impacts on soil C losses, which all affect CSE. Carbon sequestration efficiency reflects the combined magnitudes of soil heterotrophic (R_{het}) and autotrophic (R_{aut}, both below- and above-ground) respiration components, relative to GPP. We postulated that the primary effect of N_{dep} and N_{supply} is on GPP, but potential side effects of N_{dep} or N additions on ecosystem and soil carbon cycling have been postulated. The traditional theory of the role of N on microbial decomposition

715 of SOM was that, above a certain C/N threshold value, the lack of N inhibits microbial activity compared with lower C/N ratios. However, the review by Fog (1988) found that microbial activity was often unaffected, or even negatively affected, by the addition of N to low-N decomposing organic material. The negative effects were mostly found for recalcitrant organic matter (high lignin content) with a high C/N ratio (e.g. wood or straw); while N addition to easily degradable organic matter with a low C/N ratio (e.g. leaf litter with low lignin content) actually boosted microbial activity. The meta-analysis by

720 Janssens et al. (2010) of N manipulation experiments in forests suggests that excess N_r deposition reduces soil – especially heterotrophic – respiration in many temperate forests. They argue that the mechanisms include i) a decrease in below-ground C allocation and the resulting root respiration, permitted by a lesser need to develop the rooting system when more N is available (see also Alberti et al., 2015); ii) a reduction in the activity, diversity and biomass of rhizospheric mycorrhizal communities (see also Treseder, 2008); iii) a reduction in the priming effect, the stimulation of SOM decomposition by

725 saprotrophic organisms through root and mycorrhizal release of energy-rich organic compounds; iv) N-induced shifts in

saprotrophic microbial communities, leading to reduced saprotrophic respiration; and v) increased chemical stabilization of SOM into more recalcitrant compounds. The authors point out that in N-saturated forests different processes and adverse effects are at play (e.g. base cation leaching and soil acidification).

An important implication of the negative impact of N_r on soil respiration is that the nitrogen fertilisation effect on gross

730   photosynthesis would be roughly doubled, in terms of C sequestration, by the concomitant decrease in soil respiration. In their meta-analyses of N addition experiments in forests and comparison of sites exposed to low *vs* elevated N_{dep}, Janssens et al. (2010) show that both R_{het} and soil carbon efflux (SCE), a proxy for total R_{soil} (= R_{het} + $R_{aut,soil}$), tend to decline with N addition, be it through fertilisation or atmospheric deposition, although the effect is far from universal. The negative N_{dep} response of R_{het} was much more pronounced for SOM than for leaf litter, and stronger at highly productive sites than at less

735   productive sites. The negative impact on SCE was mostly found at sites where N was not limiting for photosynthesis. When N is strongly limiting, and in young forests, N_r deposition may well favour SOM decomposition.

To examine the potential impact of N_{dep} on R_{soil}, we compiled the soil respiration data available from the literature and databases for the collection of forest sites in our study, which covers the whole N limitation to N saturation spectrum. Sites ranged from highly N-limited boreal systems, where an N addition might trigger enhanced tree growth, increased microbial

740   biomass and heterotrophic respiration, to N-saturated, acidified systems (EN2, EN8, possibly also EN15, EN16), in which poor ecosystem and soil health may lead to different ecological responses than those of the below-ground carbon cycling scheme in Janssens et al. (2010).

Since the below-ground autotrophic (root and rhizosphere) respiration component is regulated by photosynthetic activity (Collalti and Prentice, 2019) and contributes a large part of R_{soil} on an annual basis (Korhonen et al., 2009), the relationship of

745   R_{soil} to N_{dep} is examined by first normalizing to GPP (Fig. 10A), yielding a soil respiration metric that is comparable between sites (for R_{soil} data, see Table S7 in the Supplement to Flechard et al., 2019). Similarly, the ratio R_{soil}/R_{eco} shows the relative contribution of below-ground to total (ecosystem) respiration (Fig. 10C). Note that caution is needed when considering both R_{soil}/GPP and R_{soil}/R_{eco} ratios, since significant uncertainty may arise from i) methodological flaws in comparing chamber *versus* eddy covariance measurements (e.g. considerations over tower footprint, spatial heterogeneity and representativeness

750   of soil collars), ii) uncertainty in deriving GPP and R_{eco} estimates from EC-NEE measurements, and iii) different time spans for the EC and soil chamber measurements, affected by inter-annual flux variability. Thus, values of R_{soil}/R_{eco} above unity (Fig. 10C), although physically non-sensical, do not necessarily imply large measurement errors, but possibly also that there may be no spatial or temporal coherence in EC and chamber data (Luyssaert et al., 2009).

Either ignoring such outliers, or judging that a measurement bias by soil chambers affects all sites the same way (e.g.

755   systematic over-estimation of soil respiration in low turbulence conditions when using static chambers, Brændholt et al., 2017), we may argue that the apparent decrease of both chamber/EC ratios R_{soil}/GPP and R_{soil}/R_{eco} with N_{dep} (Fig. 10A, 10C) has some reality, even if their absolute values are biased. Soil CO_2 efflux tends to be a larger fraction of GPP (>0.5) at the smaller N_{dep} rates (<1.5 g (N) m^{-2} yr^{-1}) than at sites with larger N_{dep}, where this fraction is more often in the range 0.4–0.5. It is also noteworthy that the largest R_{soil}/GPP ratios (EN5, EN17) are found at sites with very large SOC compared with the

760   other sites (Fig. 10B). The R_{het}/R_{soil} ratio also tends to decrease with N_{dep} (Fig. 10E), and although measured by different methods at the different sites, this is arguably a more robust metric than chamber/EC respiration ratios, because the differential respiration measurements on control and treatment plots (root exclusion, trenching, girdling) are made on the same spatial and temporal scales.

Many other factors that impact soil respiration (age, soil pH, microbial abundance and diversity, etc.) are not considered here

765   and beyond the scope of this paper. In view of these uncertainties, if the assessment within this restricted dataset does not provide a full and incontrovertible proof of the negative impact of N_r deposition on soil respiration, it at least is not in open contradiction to the prevailing paradigm that both below-ground autotrophic and heterotrophic respiration are expected to decrease as N_r deposition increases. However, the decreasing trends observed in Fig. 10A, 10C, 10E are largely driven by

these few high N_{dep} sites (>3g (N) m^{-2} yr^{-1}) in which the negative effects of N saturation and acidification very likely
770   outweigh the benefits of reduced soil respiration in terms of C sequestration.

{Insert Fig. 10 here}

5 Conclusion

The magnitude of the mean N_r deposition-induced fertilisation effect on forest C sequestration, derived here from eddy
covariance flux data from a diverse range of European forest sites, is of the order of 40–50 g (C) g^{-1} (N), and comparable with
775   the lower end of estimates obtained from inventory data and deposition rates from continental-scale deposition modelling
used in the most recent studies and reviews. The range of dC/dN values is a consequence of where in the ecosystem the N_r-
induced carbon sequestration takes place, whether there are N_r losses and how other environmental conditions affect growth.
However, this mean dC/dN response should be taken with caution for several reasons. First, uncertainties in our dC/dN
estimates are large, partly because of the relatively small number of sites (31) and their large diversity in terms of age,
780   species, climate, soils, and possibly fertility and nutrient availability. Second, adopting a mean overall dC/dN response
universally and regardless of the context may be misleading due to the clear non-linearity in the relationship between forest
productivity and the level of N_r deposition, i.e. the magnitude of the response changes with the N status of the ecosystem.
Beyond a N_r deposition threshold of 1–2 g (N) m^{-2} yr^{-1} the productivity gain per unit N_r deposited from the atmosphere starts
to decrease significantly. Above 2.5 g (N) m^{-2} yr^{-1}, productivity actually decreases with further N_r deposition additions, and
785   this is accompanied by increasingly large ecosystem N_r losses, especially as NO_3^- leaching.

Ecosystem meta-modelling was required to factor out the effects of climate, soil water retention and age on forest
productivity, a necessary step before estimating a generalised response of C storage to N_r deposition. Neglecting these effects
would lead to a large over-estimation (factor of 2) of the dC/dN effect in this European dataset and possibly also in other
datasets worldwide. After factoring out the effects of climate, soil water retention and forest age in the present dataset, only
790   part of the non-linearity was removed and there was still a decline in the dC/dN response with increasing N_{dep}. One possible
interpretation is that the remaining non-linearity may be regarded as an indicator of the impact of increasing severity of N
saturation on ecosystem functioning and forest growth. However, the results also show that the large inter-site variability in
carbon sequestration efficiency, here defined at the ecosystem scale and observed in flux data, cannot be entirely explained
by the processes represented in model we used. This is likely due in part to an incomplete understanding and over-simplified
795   model representation of plant carbon relations, soil heterotrophic and autotrophic respiration, the response to nitrogen
deposition of physiological processes such as stomatal conductance and water-use efficiency, and possibly also because other
nutrient limitations were insufficiently documented at the monitoring sites and not accounted for in the model.

Code and data availability

The data used in this study are publicly available from online databases and from the literature as described in the Materials
800   and Methods section.
The codes of models and other software used in this study are publicly available online as described in the Materials and
Methods section.

Author Contributions

CRF, MvO, DRC, WdV, MAS, AI conceived the paper; CRF performed the data analyses, ran model simulations and wrote
805   the text; MvO, DRC wrote and provided the BASFOR model code and performed Bayesian calibration; MAS, EN, UMS,
KBB, WdV conceived or designed the NEU study; AI, NB, IAJ, JN, LM, AV, DL, ALeg, KZ, MAub, MAur, BHC, JD, WE,

RJ, WLK, ALoh, BL, GM, VM, JO, MJS, TV, CV, KBB, UMS provided eddy covariance and/or other field data, or contributed to data collection from external databases and literature; MvO, DRC, WdV, AI, MAS, NB, NBD, IAJ, JN, LM, AV, DL, ALeg, KZ, AJF, RJ, AN, EN, UMS contributed substantially to discussions and revisions.

810 **Competing Interests**

The authors declare that they have no conflict of interest

Acknowledgements

The authors gratefully acknowledge financial support by the European Commission through the two FP-6 integrated projects CarboEurope-IP (Project No. GOCE-CT-2003-505572) and NitroEurope-IP (Project No. 017841), the FP-7 ECLAIRE
815 project (Grant Agreement No. 282910), and the ABBA COST Action ES0804. We are also thankful for funding from the French GIP-ECOFOR consortium under the F-ORE-T forest observation and experimentation network, and from the MDM-2017-0714 Spanish grant. We are grateful to Janne Korhonen, Mari Pihlatie and Dave Simpson for their comments on the manuscript. Finalisation of the manuscript was supported by the UK Natural Environment Research Council award number NE/R016429/1 as part of the UK-SCAPE programme delivering National Capability.

820 **References**

Alberti, G., Vicca, S., Inglima, I., Belelli-Marchesini, L., Genesio, L., Miglietta, F., Marjanovic, H., Martinez, C., Matteucci, G., D'Andrea, E., Peressotti, A., Petrella, F., Rodeghiero, M. and Cotrufo, M.F.: Soil C:N stoichiometry controls carbon sink partitioning between above-ground tree biomass and soil organic matter in high fertility forests, iForest, 8, 195-206, https://doi.org/10.3832/ifor1196-008, 2015.

825 Amiro, B.D., Barr, A.G., Barr, J.G., Black, T.A., Bracho, R., Brown, M., Chen, J., Clark, K.L., Davis, K.J., Desai, A.R., Dore, S., Engel, V., Fuentes, J.D., Goldstein, A.H., Goulden, M.L., Kolb, T.E., Lavigne, M.B., Law, B.E., Margolis, H.A., Martin, T., McCaughey, J.H., Misson, L., Montes- Helu, M., Noormets, A., Randerson, J.T., Starr, G. and Xiao, J. : Ecosystem carbon dioxide fluxes after disturbance in forests of North America, J. Geophys. Res., 115, G00K02, http://doi.org/10.1029/2010JG001390, 2010.

830 Anthoni, P.M., Knohl, A., Rebmann, C., Freibauer, A., Mund, M., Ziegler, W., Kolle, O. and Schulze, E.D.: Forest and agricultural land-use-dependent CO_2 exchange in Thuringia, Germany, Glob. Change Biol., 10, 2005–2019, https://doi.org/10.1111/j.1365-2486.2004.00863.x, 2004.

Aubinet, M.A., Grelle, A., Ibrom, A., Rannik, Ü., Moncrieff, J., Foken, T., Kowalski, T.A.S., Martin, P.H., Berbigier, P., Bernhofer, C., Clement, R., Elbers, J., Granier, A., Grünwald, T., Morgenstern, K., Pilegaard, K., Rebmann, C., Snijders, W.,
835 Valentini, R. and Vesala, T.: Estimates of the annual net carbon and water exchange of forests: The EUROFLUX methodology, Adv. Ecol. Res., 30, 113– 175, https://doi.org/10.1016/S0065-2504(08)60018-5, 2000.

BASFOR, BASic FORest ecosystem model: https://github.com/MarcelVanOijen/BASFOR, 2016.

Besnard, S., Carvalhais, N., Arain, A., Black, A., de Bruin, S., Buchmann, N., Cescatti, A., Chen, J., JClevers, J.G.P.W., Desai, A.R., Gough, C.M., Havrankova, K., Herold, M., Hörtnagl, L., Jung, M., Knohl, A., Kruijt, B., Krupkova, L., Law,
840 B.E., Lindroth, A., Noormets, A., Roupsard, O., Steinbrecher, R., Varlagin, A., Vincke, C. and Reichstein, M.: Quantifying the effect of forest age in annual net forest carbon balance, Environ. Res. Lett., 13, 124018, https://doi.org/10.1088/1748-9326/aaeaeb, 2018.

Brændholt, A., Larsen, K.S., Ibrom, A. and Pilegaard, K.: Overestimation of closed-chamber soil CO_2 effluxes at low atmospheric turbulence, Biogeosciences, 14, 1603–1616, https://doi.org/10.5194/bg-14-1603-2017, 2017.

845   Buchmann, N. and Schulze, E.-D.: Net CO_2 and H_2O fluxes of terrestrial ecosystems, Global Biogeochem. Cy., 13(3), 751–760, https://doi.org/10.1029/1999GB900016, 1999.

Burba, G.: Illustrative Maps of Past and Present Eddy Covariance Measurement Locations: II. High-Resolution Images, https://doi.org/10.13140/RG.2.2.33191.70561, 2019.

Butterbach-Bahl, K. and Gundersen, P.: Nitrogen processes in terrestrial ecosystems, in: The European Nitrogen Assessment,
850   edited by: Sutton, M., Howard, C.M., Erisman, J.W., Billen, G., Bleeker, A., Grennfelt, P., van Grinsven, H. and Grizzetti, B., Cambridge University Press, Cambridge, UK, 99–125, http://www.nine-esf.org/files/ena_doc/ENA_pdfs/ENA_c6.pdf, 2011.

Cameron, D., Flechard, C. and van Oijen, M.: Calibrating a process-based forest model with a rich observational dataset at 22 European forest sites, Biogeosciences Discuss., https://doi.org/10.5194/bg-2018-156, 2018.

855   Chapin, F.S., Woodwell, G.M., Randerson, J.T., Rastetter, E.B., Lovett, G.M., Baldocchi, D.D., Clark, D.A., Harmon, M.E., Schimel, D.S., Valentini, R., Wirth, C., Aber, J.D., Cole, J.J., Goulden, M.L., Harden, J.W., Heimann, M., Howarth, R.W., Matson, P.A., McGuire, A.D., Melillo, J.M., Mooney, H.A., Neff, J.C., Houghton, R.A., Pace, M.L., Ryan, M.G., Running, S.W., Sala, O.E., Schlesinger, W.H. and Schulze, E.-D.: Reconciling carbon-cycle concepts, terminology, and methods, Ecosystems, 9, 1041–1050, https://doi.org/10.1007/s10021-005-0105-7, 2006.

860   Chen, Z., Yu, G., Zhu, X., Wang, Q., Niu, S., Hu, Z.: Covariation between gross primary production and ecosystem respiration across space and the underlying mechanisms: a global synthesis, Agr. Forest Meteorol., 203, 180–190, 2015.

Ciais, P., Sabine, C., Bala, G., Bopp, L., Brovkin, V., Canadell, J., Chhabra, A., DeFries, R., Galloway, J., Heimann, M., Jones, C., Le Quéré, C., Myneni, R.B., Piao, S. and Thornton, P.: Carbon and Other Biogeochemical Cycles, in: Climate Change 2013: The Physical Science Basis. Contribution of Working Group I to the Fifth Assessment Report of the
865   Intergovernmental Panel on Climate Change, edited by: Stocker, T.F., Qin, D., Plattner, G.-K., Tignor, M., Allen, S.K., Boschung, J., Nauels, A., Xia, Y., Bex, V. and Midgley, P.M., Cambridge University Press, Cambridge, UK and New York, NY, USA, 465–570, https://www.ipcc.ch/report/ar5/wg1/carbon-and-other-biogeochemical-cycles/, 2013.

Collalti, A. and Prentice, I.C.: Is NPP proportional to GPP? Waring's hypothesis 20 years on, Tree Physiol., 39, 1473–1483, https://doi.org/10.1093/treephys/tpz034, 2019.

870   De Schrijver, A., Verheyen, K., Mertens, J., Staelens, J., Wuyts, K. and Muys, B.: Nitrogen saturation and net ecosystem production, Nature, 451, E1, https://doi.org/10.1038/nature06578, 2008.

De Vries, W., Solberg, S., Dobbertin, M., Sterba, H., Laubhann, D., Reinds, G.J., Nabuurs, G.J., Gundersen, P. and Sutton, M.A.: Ecologically implausible carbon response?, Nature, 451, E1–E3, https://doi.org/10.1038/nature06579, 2008.

De Vries, W., Solberg, S., Dobbertin, M., Sterba, H., Laubhann, D., van Oijen, M., Evans, C., Gundersen, P., Kros, J.,
875   Wamelink, G.W.W., Reinds, G.J. and Sutton, M.A.: The impact of nitrogen deposition on carbon sequestration by European forests and heathlands, Forest Ecol. Manag., 258, 1814–1823, https://doi.org/10.1016/j.foreco.2009.02.034, 2009.

De Vries, W., Du, E. and Butterbach-Bahl, K.: Short and long-term impacts of nitrogen deposition on carbon sequestration by forest ecosystems, Curr. Opin. Env. Sust., 9–10, 90–104, https://doi.org/10.1016/j.cosust.2014.09.001, 2014.

Dezi, S., Medlyn, B.E., Tonon, G. and Magnani, F.: The effect of nitrogen deposition on forest carbon sequestration: a
880   model-based analysis, Glob. Change Biol., 16, 1470–1486, https://doi.org/10.1111/j.1365-2486.2009.02102.x, 2010.

Dorn, J.: Matlab «*distributionPlot*.m» function, https://fr.mathworks.com/matlabcentral/fileexchange/23661-violin-plots-for-plotting-multiple-distributions-distributionplot-m?s_tid=prof_contriblnk, 2008.

Erisman, J.W., Galloway, J., Seitzinger, S., Bleeker, A. and Butterbach-Bahl, K.: Reactive nitrogen in the environment and its effect on climate change, Curr. Opin. Env. Sust., 3(5), 281–290, https://doi.org/10.1016/j.cosust.2011.08.012, 2011.

885   Etzold, S., Waldner, P., Thimonier, A., Schmitt, M. and Dobbertin, M.: Tree growth in Swiss forests between 1995 and 2010 in relation to climate and stand conditions: recent disturbances matter, Forest Ecol. Manag., 311, 41–55, https://doi.org/10.1016/j.foreco.2013.05.040, 2014.

European Fluxes Database Cluster : http://www.europe-fluxdata.eu/, 2012.

Falge, E., Baldocchi, D., Olson, R., Anthoni, P., Aubinet, M., Bernhofer, C., Burba, G., Ceulemans, R., Clement, R., Dolman, H., Granier, A., Gross, P., Grunwald, T., Hollinger, D., Jensen, N.O., Katul, G., Keronen, P., Kowalski, A., Lai, C.T., Law, B.E., Meyers,T., Moncrieff, H., Moors, E., Munger, J.W., Pilegaard, K., Rannik,U., Rebmann, C., Suyker, A., Tenhunen, J., Tu, K., Verma, S., Vesala, T., Wilson, K. and Wofsy, S.: Gap filling strategies for defensible annual sums of net ecosystem exchange, Agr. Forest Meteorol., 107, 43–69, https://doi.org/10.1016/S0168-1923(00)00225-2, 2001.

Fernández-Martínez, M., Vicca, S., Janssens, I.A., Sardans, J., Luyssaert, S., Campioli, M., Chapin, F.S., Ciais, P., Malhi, Y., Obersteiner, M., Papale, D., Piao, S.L., Reichstein, M., Rodà, F. and Peñuelas, J: Nutrient availability as the key regulator of global forest carbon balance, Nat. Clim. Change, 4, 471–476, https://doi.org/10.1038/nclimate2177, 2014.

Fernández-Martínez, M., Vicca, S., Janssens, I.A., Sardans, J., Luyssaert, S., Campioli, M., Chapin, F.S., Ciais, P., Malhi, Y., Oberteiner, M., Papale, D., Piao, S.L., Reichstein, M., Rodà, F. and Peñuelas, J : Reply to 'Uncertain effects of nutrient availability on global forest carbon balance' and 'Data quality and the role of nutrients in forest carbon-use efficiency', Nat. Clim. Change, 5, 960–961, https://doi.org/10.1038/nclimate2794, 2015.

Fernández-Martínez, M., Vicca, S., Janssens, I.A., Ciais, P., Obersteiner, M., Bartrons, M., Sardans, J., Verger, A., Canadell, J.G., Chevallier, F., Wang, X., Bernhofer, C., Curtis, P.S., Gianelle, D., Gruwald, T., Heinesch, B., Ibrom, A., Knohl, A., Laurila, T., Law, B.E., Limousin, J.M., Longdoz, B., Loustau, D., Mammarella, I., Matteucci, G., Monson, R.K., Montagnani, L., Moors, E.J., Munger, J.W., Papale, D., Piao, S.L. and Penuelas, J.: Atmospheric deposition, CO_2, and change in the land carbon sink, Sci. Rep.-UK, 7, 9632, https://doi.org/DOI:10.1038/s41598-017-08755-8, 2017.

Finzi, A.C., Norby, R.J., Calfapietra, C., Gallet-Budynek, A., Gielen, B., Holmes, W.E., Hoosbeek, M.R., Iversen, C.M., Jackson, R.B., Kubiske, M.E., Ledford, J., Liberloo, M., Oren, R., Polle, A., Pritchard, S., Zak, D.R., Schlesinger, W.H. and Ceulemans, R.: Increases in nitrogen uptake rather than nitrogen-use efficiency support higher rates of temperate forest productivity under elevated CO_2, P. Natl. Acad. Sci. USA, 104(35), 14014–14019, https://doi.org/10.1073/pnas.0706518104, 2007.

Flechard C.R., Nemitz E., Smith R.I., Fowler D., Vermeulen A.T., Bleeker A., Erisman J.W., Simpson D., Zhang L., Tang Y.S. and Sutton M.A.: Dry deposition of reactive nitrogen to European ecosystems: a comparison of inferential models across the NitroEurope network, Atmos. Chem. Phys., 11, 2703–2728, https://doi.org/10.5194/acp-11-2703-2011, 2011.

Flechard, C.R., Ibrom, A., Skiba, U.M., de Vries, W., van Oijen, M., Cameron, D.R., Dise, N.B., Korhonen, J.F.J., Buchmann, N., Legout, A., Simpson, D., Sanz, M.J., Aubinet, M., Loustau, D., Montagnani, L., Neirynck, J., Janssens, I.A., Pihlatie, M., Kiese, R., Siemens, J., Francez, A.-J., Augustin, J., Varlagin, A., Olejnik, J., Juszczak, R., Aurela, M., Chojnicki, B.H., Dämmgen, U., Djuricic, V., Drewer, J., Eugster, W., Fauvel, Y., Fowler, D., Frumau, A., Granier, A., Gross, P., Hamon, Y., Helfter, C., Hensen, A., Horváth, L., Kitzler, B., Kruijt, B., Kutsch, W.L., Lobo-do-Vale, R., Lohila, A., Longdoz, B., Marek, M.V., Matteucci, G., Mitosinkova, M., Moreaux, V., Neftel, A., Ourcival, J.-M., Pilegaard, K., Pita, G., Sanz, F., Schjoerring, J.K., Sebastià, M.T., Tang, Y.S., Uggerud, H., Urbaniak, M., van Dijk, N., Vesala, T., Vidic, S., Vincke, C., Weidinger, T., Zechmeister-Boltenstern, S., Butterbach-Bahl, K., Nemitz, E and Sutton, M.A.: Carbon / nitrogen interactions in European forests and semi-natural vegetation. Part I: Fluxes and budgets of carbon, nitrogen and greenhouse gases from ecosystem monitoring and modelling, Biogeosciences Discuss., submitted, 2019.

Fleischer, K., Rebel, K.T., Van Der Molen, M.K., Erisman, J.W., Wassen, M.J., van Loon, E.E., Montagnani, L., Gough, C.M., Herbst, M., Janssens, I.A., Gianelle, D. and Dolman, A.J.: The contribution of nitrogen deposition to the photosynthetic capacity of forests, Global Biogeochem. Cy., 27, 187–199, https://doi.org/10.1002/gbc.20026, 2013.

Fog, K.: The effect of added nitrogen on the rate of decomposition of organic matter, Biol. Rev., 63, 433–462, https://doi.org/10.1111/j.1469-185X.1988.tb00725.x, 1988.

Fowler, D., Steadman, C.E., Stevenson, D., Coyle, M., Rees, R.M., Skiba, U.M., Sutton, M.A., Cape, J.N., Dore, A.J., Vieno, M., Simpson, D., Zaehle, S., Stocker, B.D., Rinaldi, M., Facchini, M.C., Flechard, C., Nemitz, E., Twigg, M., Erisman, J.W., Butterbach-Bahl, K. and Galloway, J.N.: Effects of global change during the 21st century on the nitrogen cycle, Atmos. Chem. Phys., 15 (24), 13849-13893, https://doi.org/10.5194/acp-15-13849-2015, 2015.

Granier, A., Breda, N., Longdoz, B., Gross, P. and Ngao, J.: Ten years of fluxes and stand growth in a young beech forest at Hesse, North-eastern France, Ann. For. Sci., 64, 704, https://doi.org/10.1051/forest:2008052, 2008.

935 Gundale, M.J., From, F., Back-Holmen, L. and Nordin, A.: Nitrogen deposition in boreal forests has a minor impact on the global carbon cycle, Glob. Change Biol., 20, 276–286, https://doi.org/10.1111/gcb.12422, 2014.

Högberg, P.: Nitrogen impacts on forest carbon, Nature, 447, 781–782, https://doi.org/10.1038/447781a, 2007.

Högberg, P.: What is the quantitative relation between nitrogen deposition and forest carbon sequestration?, Glob. Change Biol., 18, 1–2, https://doi.org/10.1111/j.1365-2486.2011.02553.x, 2012.

940 Holmberg, M., Aherne, J., Austnes, K., Beloica, J., De Marco, A., Dirnböck, T., Fornasier, M.F., Goergen, K., Futter, M., Lindroos, A.-J., Krám, P., Neirynck, J., Nieminen, T.M., Pecka, T., Posch, M., Pröll, G., Rowe, E.C., Scheuschner, T., Schlutow, A., Valinia, S. and Forsius, M.: Modelling study of soil C, N and pH response to air pollution and climate change using European LTER site observations, Sci. Total Environ., 640–641, 387–399, https://doi.org/10.1016/j.scitotenv.2018.05.299, 2018.

945 ICP, International Co-operative Programme on Assessment and Monitoring of Air Pollution Effects on Forests: http://icp-forests.net/, 2019.

Janssens, I.A., Sampson, D.A., Cermak, J., Meiresonne, L., Riguzzi, F., Overloop, S. and Ceulemans, C. : Above-and belowground phytomass and carbon storage in a Belgian Scots pine stand, Ann. For. Sci., 56 (2), 81–90, https://doi.org/10.1051/forest:19990201, 1999.

950 Janssens, I.A., Lankreijer, H., Matteucci, G., Kowalski, A.S., Buchmann, N., Epron, D., Pilegaard, K., Kutsch, W., Longdoz, B., Grünwald, T., Montagnani, L., Dore, S., Rebmann, C., Moors, E.J., Grelle, A., Rannik, Ü., Morgenstern, K., Oltchev, S., Clement, R., Guðmundsson, J., Minerbi, S., Berbigier, P., Ibrom, A., Moncrieff, J., Aubinet, M., Bernhofer, C., Jensen, N.O., Vesala, T., Granier, A., Schulze, E.- D., Lindroth, A., Dolman, A.J., Jarvis, P.G., Ceulemans, R. and Valentini, R.: Productivity overshadows temperature in determining soil and ecosystem respiration across European forests, Glob. Change

955 Biol., 7, 269–278, https://doi.org/10.1046/j.1365-2486.2001.00412.x, 2001.

Janssens, I.A., Dieleman, W., Luyssaert, S., Subke, J., Reichstein, M., Ceulemans, R., Ciais,P., Dolman, A.J., Grace, J. and Matteucci, G., Papale, D., Piao, S.L., Schulze, E-D., Tang, J. and Law, B.E.: Reduction of forest soil respiration in response to nitrogen deposition, Nat. Geosci., 3, 315–322, https://doi.org/10.1038/ngeo844, 2010.

Kolari, P., Pumpanen, J., Rannik, Ü., Ilvesniemi, H., Hari, P. and Berninger, F.: Carbon balance of different aged Scots pine

960 forests in Southern Finland, Glob. Change Biol., 10, 1106–1119, https://doi.org/10.1111/j.1529-8817.2003.00797.x, 2004.

Kreutzer, K., Butterbach-Bahl, K., Rennenberg, H. and Papen, H.: The complete nitrogen cycle of an N-saturated spruce forest ecosystem, Plant Biol., 11, 643–649, https://doi.org/10.1111/j.1438-8677.2009.00236.x, 2009.

Kutsch, W.L. and Kolari, P.: Data quality and the role of nutrients in forest carbon-use efficiency, Nat. Clim. Change, 5, 959–960, https://doi.org/10.1038/nclimate2793, 2015.

965 Lasslop, G., Reichstein, M., Papale, D., Richardson, A.D., Arneth, A., Barr, A., Stoy, P. and Wohlfahrt, G.: Separation of net ecosystem exchange into assimilation and respiration using a light response curve approach: critical issues and global evaluation, Glob. Change Biol., 16, 187–208, https://doi.org/10.1111/j.1365-2486.2009.02041.x, 2010.

LeBauer, D.S. and Treseder, K.K.: Nitrogen limitation of net primary productivity in terrestrial ecosystems is globally distributed, Ecology, 89, 371–379, https://doi.org/10.1890/06-2057.1, 2008.

970 Lee, X., Massman, W. and Law, B. (Eds.): Handbook of micrometeorology. A guide for surface flux measurement and analysis, Atmos. Ocean. Sci. Lib., 29, ISBN 1-4020-2264-6, Kluwer Academic Publishers, Dordrecht, 250 pp., 2004.

Liu, L. and Greaver, T.L.: A review of nitrogen enrichment effects on three biogenic GHGs: the CO_2 sink may be largely offset by stimulated N_2O and CH_4 emission, Ecol. Lett., 12 (10), 1103–1117, https://doi.org/10.1111/j.1461-0248.2009.01351.x, 2009.

975 Luyssaert, S., Schulze, E.-D., Börner, A., Knohl, A., Hessenmöller, D., Law, B.E., Ciais, P. and Grace, J.: Old-growth forests as global carbon sinks, Nature, 455, 213–215, http://doi.org/10.1038/nature07276, 2008.

Luyssaert, S., Reichstein, M., Schulze, E- D., Janssens, I.A., Law, B.E., Papale, D., Dragoni, D., Goulden, M.L., Granier, A., Kutsch, W.L., Linder, S., Matteucci, G., Moors, E., Munger, J.W., Pilegaard, K., Saunders, M., Falge, E.M.: Toward a consistency crosscheck of eddy covariance flux-based and biometric estimates of ecosystem carbon balance, Global
980   Biogeochem. Cy., 23, GB3009, http://doi.org/10.1029/2008GB003377, 2009.

Lovett, G.M., Arthur, M.A., Weathers, K.C., Fitzhugh, R.D. and Templer, P.H.: Nitrogen addition increases carbon storage in soils, but not in trees, in an Eastern U.S. deciduous forest, Ecosystems, 16, 980–1001, https://doi.org/10.1007/s10021-013-9662-3, 2013.

Magnani, F., Mencuccini, M., Borghetti, M., Berbigier, P., Berninger, F., Delzon, S., Grelle, A., Hari, P., Jarvis, P.G., Kolari,
985   P., Kowalski, A.S., Lankreijer, H., Law, B.E., Lindroth, A., Loustau, D., Manca, G., Moncrieff, J.B., Rayment, M., Tedeschi, V., Valentini, R. and Grace, J.: The human footprint in the carbon cycle of temperate and boreal forests, Nature, 447, 848–850, https://doi.org/doi:10.1038/nature05847, 2007.

Magnani, F., Mencuccini, M., Borghetti, M., Berninger, F., Delzon, S., Grelle, A., Hari, P., Jarvis, P.G., Kolari, P., Kowalski, A.S., Lankreijer, H., Law, B.E., Lindroth, A., Loustau, D., Manca, G., Moncrieff, J.B., Tedeschi, V., Valentini, R. and Grace,
990   J.: Reply to A. De Schrijver et al. (2008) and W. de Vries et al. (2008), Nature, 451, E3–E4, https://doi.org/10.1038/nature06580, 2008.

Mahecha, M.D., Reichstein, M., Carvalhais, N., Lasslop, G., Lange, H., Seneviratne, S.I., Vargas, R., Ammann, C., Arain, M.A., Cescatti, A., Janssens, I.A., Migliavacca, M., Montagnani, L. and Richardson, A.D.: Global convergence in the temperature sensitivity of respiration at ecosystem level, Science, 329, 838–840, https://doi.org/10.1126/science.1189587,
995   2010.

Migliavacca, M., Reichstein, M., Richardson, A.M., Colombo, R., Sutton, M.A., Lasslop, G., Tomelleri, E., Wohlfahrt, G., Carvalhais, N., Cescatti, A., Mahecha, M.D., Montagnani, L., Papale, D., Zaehle, S., Arain, A., Arneth, A., Black, T.A., Carrara, A., Dore, S., Gianelle, D., Helfter, C., Hollinger, D., Kutsch, W.L., Lafleur, P.M., Nouvellon, Y., Rebmann, C., Da Rocha, H.R., Rodeghiero, M., Roupsard, O., Sebastià, M.T., Seufert, G., Soussana, J.-F. and Van Der Molen, M.K.:
1000   Semiempirical modeling of abiotic and biotic factors controlling ecosystem respiration across eddy covariance sites, Glob. Change Biol., 17, 390–409, https://doi.org/10.1111/j.1365-2486.2010.02243.x, 2011.

Nadelhoffer, K.J., Emmett, B.A., Gundersen, P., Kjønaas, O.J., Koopmansk, C.J., Schleppi, P., Tietemak, A. and Wright, R.F.: Nitrogen deposition makes a minor contribution to carbon sequestration in temperate forests, Nature, 398, 145–148, https://doi.org/10.1038/18205, 1999.

1005   Neirynck, J., Van Ranst, E., Roskams, P. and Lust, N.: Impact of declining throughfall depositions on soil solution chemistry at coniferous forests in northern Belgium, Forest Ecol. Manag., 160, 127–142, https://doi.org/10.1016/S0378-1127(01)00476-5, 2002.

Neirynck, J., Kowalski, A.S., Carrara, A., Genouw, G., Berghmans, P. and Ceulemans, R.: Fluxes of oxidised and reduced nitrogen above a mixed coniferous forest exposed to various nitrogen emission sources, Environ. Pollut., 149, 31–43,
1010   https://doi.org/10.1016/j.envpol.2006.12.029, 2007.

Neirynck, J., Flechard, C.R. and Fowler, D.: Long-term (13 years) measurements of SO$_2$ fluxes over a forest and their control by surface chemistry, Agr. Forest Meteorol., 151, 1768-1780, https://doi.org/10.1016/j.agrformet.2011.07.013, 2011.

NEU, NitroEurope Integrated Project: http://www.nitroeurope.eu/, 2013.

Odum, E.P.: The strategy of ecosystem development, Science 164(3877), 262–270, https://doi.org/
1015   10.1126/science.164.3877.262, 1969.

Reay, D.S., Dentener, F., Smith, P., Grace, J. and Feely, R.A.: Global nitrogen deposition and carbon sinks, Nat. Geosci., 1, 430–437, http://doi.org/10.1038/ngeo230, 2008.

Reichstein, M., Falge, E., Baldocchi, D., Papale, D., Aubinet, M., Berbigier, P., Bernhofer, C., Buchmann, N., Gilmanov, T., Granier, A., Grünwald, T., Havránková, K., Ilvesniemi, H., Janous, D., Knohl, A., Laurila, T., Lohila, A., Loustau, D.,
1020   Matteucci, G., Meyers, T., Miglietta, F., Ourcival, J.-M., Pumpanen, J., Rambal, S., Rotenberg, E., Sanz, M., Tenhunen, J.,

Seufert, G., Vaccari, F., Vesala, T., Yakir, D. and Valentini, R.: On the separation of net ecosystem exchange into assimilation and ecosystem respiration: review and improved algorithm, Glob. Change Biol., 11, 1424–1439, https://doi.org/10.1111/j.1365-2486.2005.001002.x, 2005.

Schulte-Uebbing, L. and de Vries, W.: Global-scale impacts of nitrogen deposition on tree carbon sequestration in tropical, temperate and boreal forests: A meta-analysis, Glob. Change Biol., 24, 416–431, https://doi.org/10.1111/gcb.13862, 2018.

Schulze, E.-D., Ciais, P., Luyssaert, S., Schrumpf, M., Janssens, I.A., Thiruchittampalam, B., Theloke, J., Saurat, M., Bringezu, S., Lelieveld, J., Lohila, A., Rebmann, C., Jung, M., Bastviken, D., Abril, G., Grassi, G., Leip, A., Freibauer, A., Kutsch, W., Don, A., Nieschulze, J., Börner, A., Gash, J.H. and Dolman, A.J.: The European carbon balance. Part 4: integration of carbon and other trace-gas fluxes, Glob. Change Biol., 16, 1451–1469, https://doi.org/10.1111/j.1365-2486.2010.02215.x, 2010.

Schwede, D.B., Simpson, D., Tan, J., Fu, J.S., Dentener, F., Du, E. and de Vries, W. : Spatial variation of modelled total, dry and wet nitrogen deposition to forests at global scale, Enviro. Pollut., 243, 1287–1301, https://doi.org/10.1016/j.envpol.2018.09.084, 2018.

Simpson, D., Benedictow, A., Berge, H., Bergström, R., Emberson, L.D., Fagerli, H., Flechard, C.R., Hayman, G.D., Gauss, M., Jonson, J.E., Jenkin, M.E., Nyíri, A., Richter, C., Semeena, V.S., Tsyro, S., Tuovinen, J.-P., Valdebenito, Á. and Wind, P.: The EMEP MSC-W chemical transport model – technical description, Atmos. Chem. Phys., 12, 7825–7865, https://doi.org/10.5194/acp-12-7825-2012, 2012.

Simpson, D., Andersson, C., Christensen, J.H., Engardt, M., Geels, C., Nyiri, A., Posch, M., Soares, J., Sofiev, M., Wind, P. and Langner, J.: Impacts of climate and emission changes on nitrogen deposition in Europe: a multi-model study, Atmos. Chem. Phys., 14, 6995–7017, https://doi.org/10.5194/acp-14-6995-2014, 2014.

Spelling, J.: Matlab «*drawSankey.m*» function, http://www.sourcecodeonline.com/author/james_spelling.html, KTH, Sweden, 2009.

Sutton, M.A., Simpson, D., Levy, P.E., Smith, R.I., Reis, S., van Oijen, M. and de Vries, W.: Uncertainties in the relationship between atmospheric nitrogen deposition and forest carbon sequestration, Glob. Change Biol., 14, 2057–2063, https://doi.org/10.1111/j.1365-2486.2008.01636.x, 2008.

Tang, J., Luyssaert, S., Richardson, A.D., Kutsch, W. and Janssens, I.A.: Steeper declines in forest photosynthesis than respiration explain age-driven decreases in forest growth, P. Natl. Acad. Sci. USA, 111, 8856–60, https://doi.org/10.1073/pnas.1320761111, 2014.

Tang, Y.S., Simmons, I., van Dijk, N., Di Marco, C., Nemitz, E., Dämmgen, U., Gilke, K., Djuricic, V., Vidic, S., Gliha, Z., Borovecki, D., Mitosinkova, M., Hanssen, J.E., Uggerud, T.H., Sanz, M.J., Sanz, P., Chorda, J.V., Flechard, C.R., Fauvel, Y., Ferm, M., Perrino, C. and Sutton, M.A.: European scale application of atmospheric reactive nitrogen measurements in a low-cost approach to infer dry deposition fluxes, Agr. Ecosyst. Environ., 133, 183–195, https://doi.org/10.1016/j.agee.2009.04.027, 2009.

Thomas, R.Q., Canham, C.D., Weathers, K.C. and Goodale, C.L.: Increased tree carbon storage in response to nitrogen deposition in the US, Nat. Geosci., 3(1), 13–17, https://doi.org/10.1038/ngeo721, 2010.

Treseder, K.K.: Nitrogen additions and microbial biomass: a meta-analysis of ecosystem studies, Ecol. Lett., 11, 1111–1120, https://doi.org/10.1111/j.1461-0248.2008.01230.x, 2008.

van Oijen, M., Rougier, J. and Smith, R.: Bayesian calibration of process-based forest models: bridging the gap between models and data, Tree Physiol., 25, 915–927, https://doi.org/10.1093/treephys/25.7.915, 2005.

Vergutz, L., Manzoni, S., Porporato, A., Ferreira Novais, R. and Jackson, R.B.: Global resorption efficiencies and concentrations of carbon and nutrients in leaves of terrestrial plants, Ecol. Monogr., 82(2), 205–220, https://doi.org/10.1890/11-0416.1, 2012.

Vicca, S., Luyssaert, S., Peñuelas, J., Campioli, M., Chapin, F.S., Ciais, P., Heinemeyer, A., Högberg, P., Kutsch, W.L., Law, B.E., Malhi, Y., Papale, D., Piao, S.L., Reichstein, M., Schulze, E.D. and I.A. Janssens: Fertile forests produce biomass more efficiently, Ecol. Lett., 15, 520–526, https://doi.org/10.1111/j.1461-0248.2012.01775.x, 2012.

Vitousek, P.M., Cassman, K., Cleveland, C., Crews, T., Field, C.B., Grimm, N.B., Horwarth, R.W., Marino, R., Martinelli, L., Rastetter, E.B. and Sprent, J.: Towards an ecological understanding of biological nitrogen fixation, Biogeochemistry, 57, 1–45, https://doi.org/10.1023/A:1015798428743, 2002.

Wang, L., Ibrom, A., Korhonen, J.F.J., Frumau, K.F.A., Wu, J., Pihlatie, M. and Schjørring, J.K.: Interactions between leaf nitrogen status and longevity in relation to N cycling in three contrasting European forest canopies, Biogeosciences, 10, 999–1011, https://doi.org/10.5194/bg-10-999-2013, 2013.

Wortman, E., Tomaszewski, T., Waldner, P., Schleppi, P., Thimonier, A., Eugster, W., Buchmann, N. and Sievering, H.: Atmospheric nitrogen deposition and canopy retention influences on photosynthetic performance at two high nitrogen deposition Swiss forests, Tellus B, 64, 17216, https://doi.org/10.3402/tellusb.v64i0.17216, 2012.

Zaehle, S. and Dalmonech, D.: Carbon–nitrogen interactions on land at global scales: current understanding in modelling climate biosphere feedbacks, Curr. Opin. Env. Sust., 3, 311-320, https://doi.org/10.1016/j.cosust.2011.08.008, 2011.

1080   **Figures and Tables**
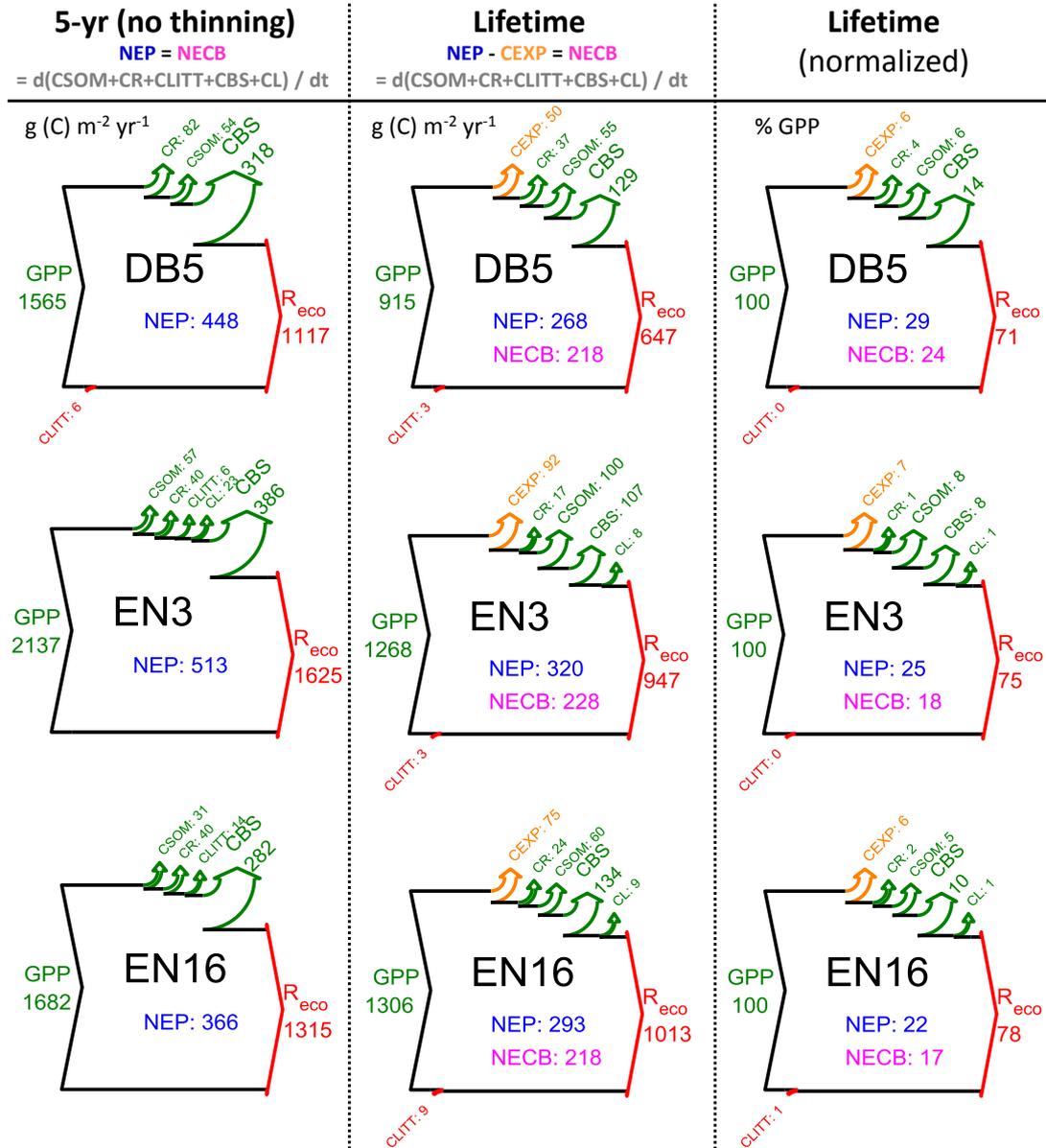
Figure 1. Modelled (BASFOR) partitioning of C fluxes at three example forest sites (DB5: 45-yr old *Fagus sylvatica*; EN3: 120-yr old *Picea abies*; EN16: 51-yr old *Pseudotsuga menziesii*), and associated modelled changes in C pools in soil organic matter (CSOM), roots (CR), litter layers (CLITT), branches and stems (CBS) and leaves (CL) (units: g (C) m^{-2} yr^{-1} left and center;

1085   normalized to % lifetime GPP on the right). Simulations were run either over the most recent 5-year period which did not include any thinning event («5-yr» in the text), or over the whole time period since the forest was established («lifetime»). Green indicates ecosystem C gain (photosynthesis and C pool increase); red denotes ecosystem C loss (respiration and C pool decrease); the orange arrows indicate C export through thinning. The NECB percentage value (right) corresponds to the lifetime carbon sequestration efficiency (CSE). The sizes of the Sankey plots are not proportional to the C fluxes of the different study sites.

1090

5-yr (no thinning) | **Lifetime** | **Lifetime** (normalized)

$$N_{supply} = N_{miner} + N_{dep} = N_{upt} + N_{leach} + N_{emission}$$

Flux units: g (N) m^{-2} yr^{-1}

Flux units: g (N) m^{-2} yr^{-1}

Flux units: % N$_{supply}$

DB5 — N_{leach}: 0.8; $N_{emission}$: 0.2; N_{miner} 8.3; NMIN 2.3 g (N) m^{-2}; N_{upt} 29.1; N_{dep} 1.8

DB5 — N_{leach} 3.5; $N_{emission}$: 0.9; N_{miner} 7.5; NMIN 10.6 g (N) m^{-2}; N_{upt} 5.5; N_{dep} 2.4

DB5 — N_{leach} 35.4; $N_{emission}$: 9.1; N_{miner} 76.0; NMIN 10.6 g (N) m^{-2}; N_{upt} 55.5; N_{dep} 24.0

EN3 — N_{leach}: 0.9; $N_{emission}$: 0.2; N_{miner} 7.0; NMIN 1.1 g (N) m^{-2}; N_{upt} 8.2; N_{dep} 2.3

EN3 — N_{leach} 1.1; $N_{emission}$: 0.1; N_{miner} 5.0; NMIN 0.7 g (N) m^{-2}; N_{upt} 5.7; N_{dep} 1.9

EN3 — N_{leach} 15.7; $N_{emission}$: 2.0; N_{miner} 73.0; NMIN 0.7 g (N) m^{-2}; N_{upt} 82.3; N_{dep} 27.0

EN16 — N_{leach} 3.9; $N_{emission}$: 0.3; N_{miner} 7.7; NMIN 2.1 g (N) m^{-2}; N_{upt} 8.1; N_{dep} 4.6

EN16 — N_{leach} 6.8; $N_{emission}$: 0.4; N_{miner} 7.8; NMIN 2.7 g (N) m^{-2}; N_{upt} 6.6; N_{dep} 6.0

EN16 — N_{leach} 48.9; $N_{emission}$: 2.6; N_{miner} 56.6; NMIN 2.7 g (N) m^{-2}; N_{upt} 48.5; N_{dep} 43.4

Figure 2. Modelled (BASFOR) nitrogen budgets at three example forest sites (DB5: 45-yr old *Fagus sylvatica*; EN3: 120-yr old *Picea abies*; EN16: 51-yr old *Pseudotsuga menziesii*). Simulations were run either over the most recent 5-year period which did not include any thinning event («5-yr» in the text), or over the whole time period since the forest was established («lifetime»). The data show ecosystem SOM mineralisation (N$_{miner}$) and atmospheric N$_r$ deposition (N$_{dep}$), balanced by vegetation uptake (N$_{upt}$) and the sum of losses as dissolved N (N$_{leach}$) and gaseous NO + N$_2$O (N$_{emission}$) (units: g (N) m^{-2} yr^{-1} left and center; % of lifetime N$_{supply}$ on the right, with N$_{supply}$ defined as N$_{miner}$ + N$_{dep}$). NMIN indicates the mean size of the soil inorganic N pool (g (N) m^{-2}) over the modelling period. The N uptake percentage value (right) corresponds to the lifetime nitrogen use efficiency (NUE). The sizes of the Sankey plots are not proportional to the N fluxes of the different study sites.

1095

1100
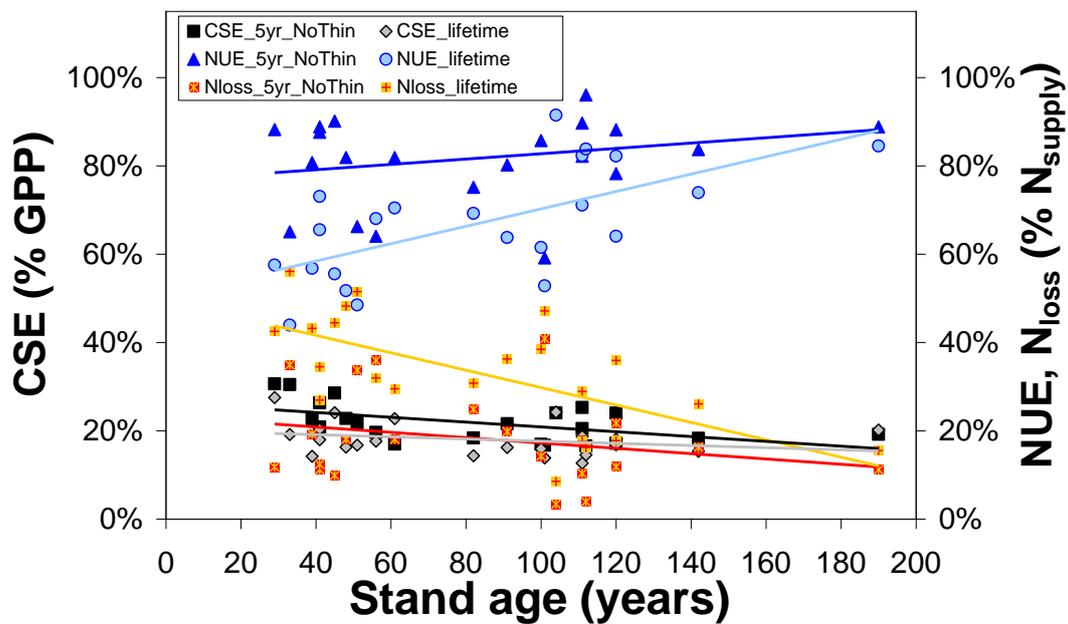
Figure 3. Influence of forest stand age on modelled (BASFOR) C sequestration efficiency (CSE, expressed as % GPP), N use efficiency (NUE) and the N_{loss} fraction (% N_{supply}). Each data point represents one of 22 modelled forest sites. CSE and NUE are calculated either i) over the most recent 5-year period including no thinning event around the time frame of the CEIP/NEU projects, or ii) over the whole lifetime of the stands (including all thinning events). See Eq. (1)-(9) for definitions and calculations of the indicators.
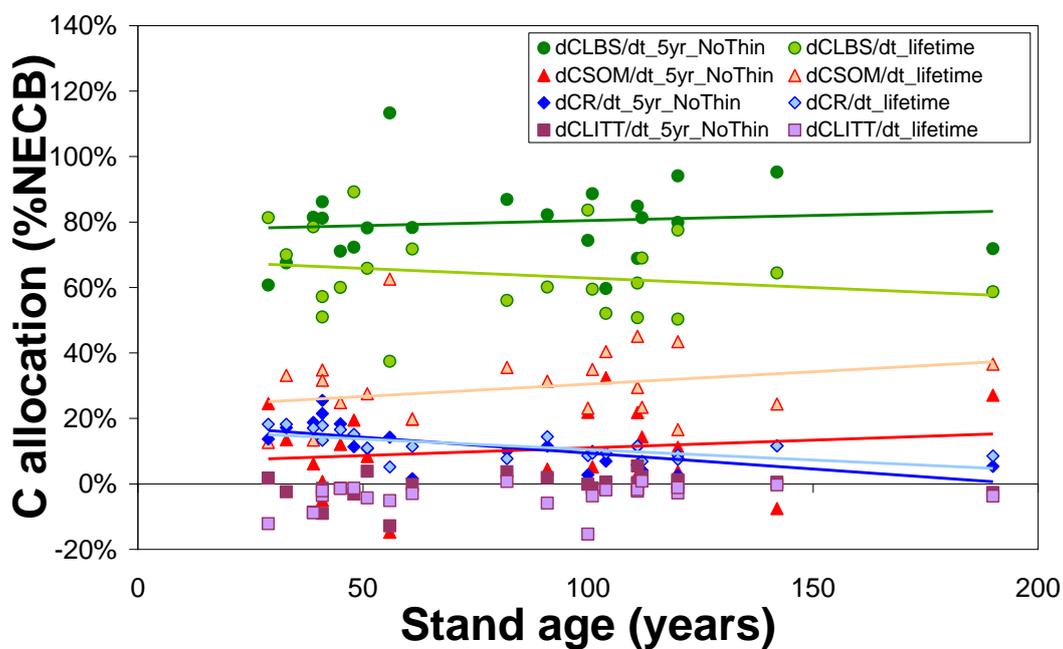
Figure 4. Modelled (BASFOR) ultimate allocation of sequestered C (as % NECB) into pools in soil organic matter (CSOM), roots (CR), litter layers (CLITT), leaves, branches and stems (CLBS). Each data point represents one of 22 modelled forest sites, plotted as a function of stand age.
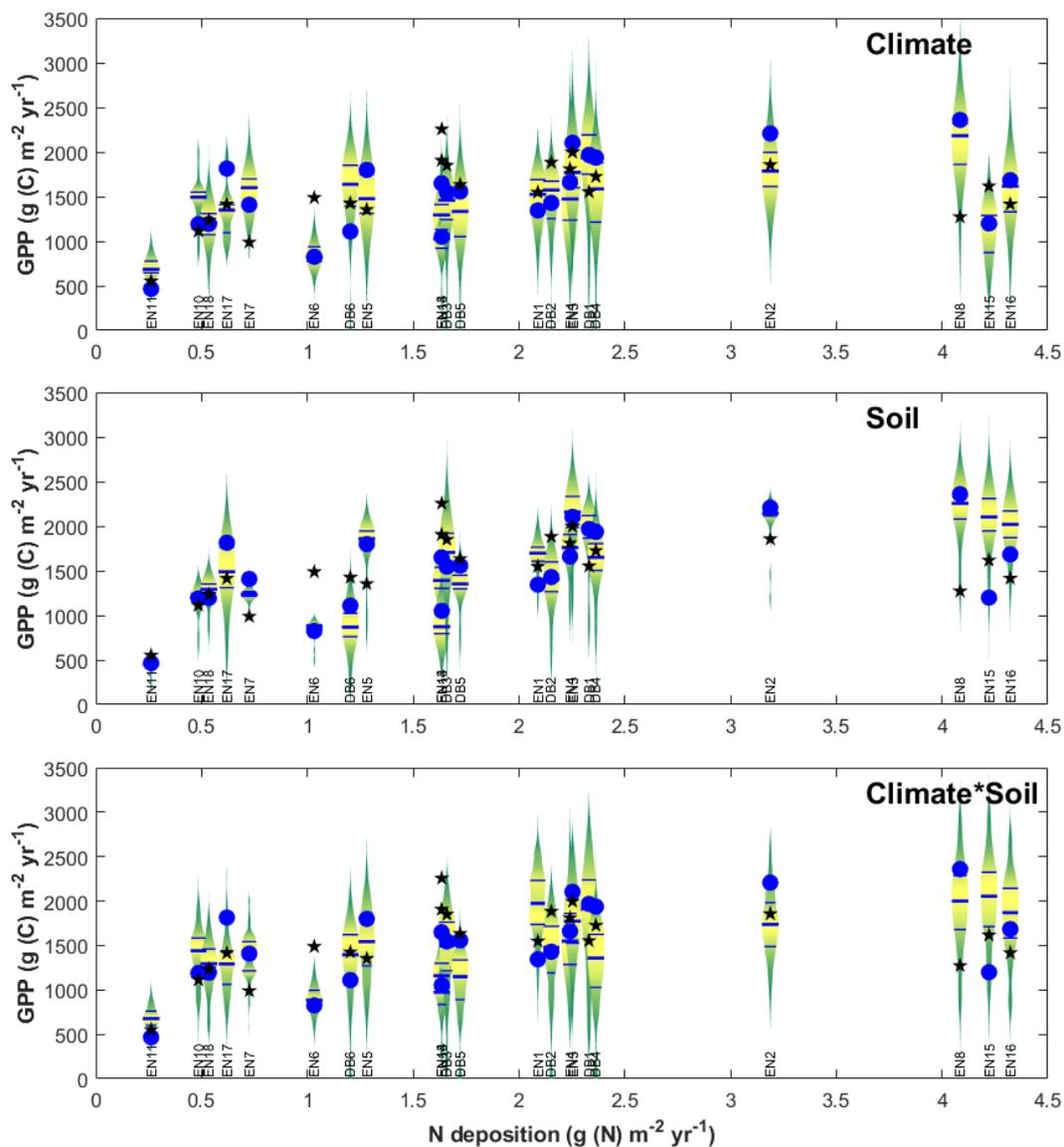
Figure 5. Comparison of distributions of gross primary productivity (GPP) at each forest monitoring site for modelled soil/climate scenarios (vertical «violin» plots), versus model base runs GPP$_{base}$ (blue circles) and EC-derived GPP$_{obs}$ (black stars). The data are displayed as a function of N$_r$ deposition over the CEIP-NEU measurement periods, for n=22 deciduous broadleaf and coniferous evergreen needleleaf forest ecosystems. See text for details.
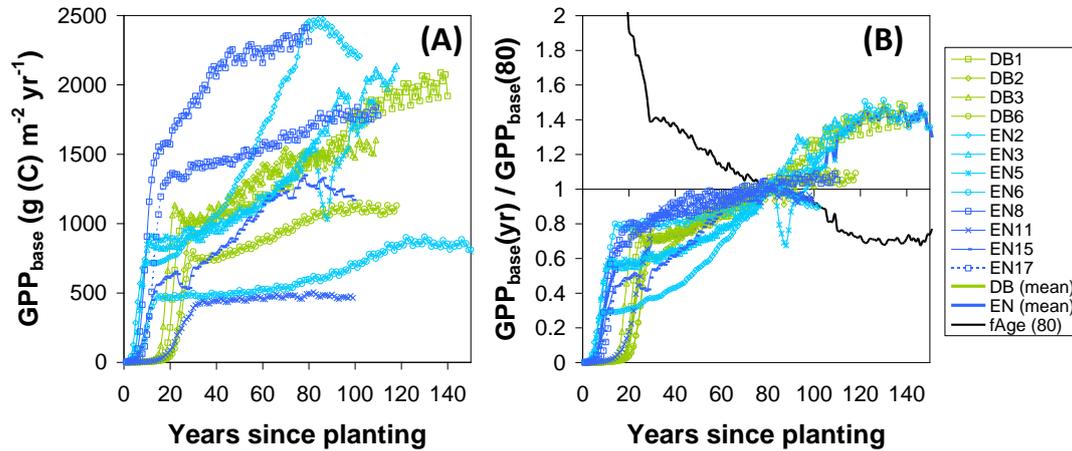
Figure 6. Calculation of f_{AGE} (normalized to 80 yr) from modelled BASFOR growth curves for mature forests (12 sites older than 80 yr). (A) Modelled (baseline) gross primary productivity (GPP_{base}); (B) Each site's GPP_{base} curve is normalized to the value at 80 yr. A single f_{AGE} curve is then calculated as the mean of all sites after normalization to $GPP_{base}(80)$ (see Eq. (16)-(17)). DB: deciduous broadleaf; EN: coniferous evergreen needleleaf.
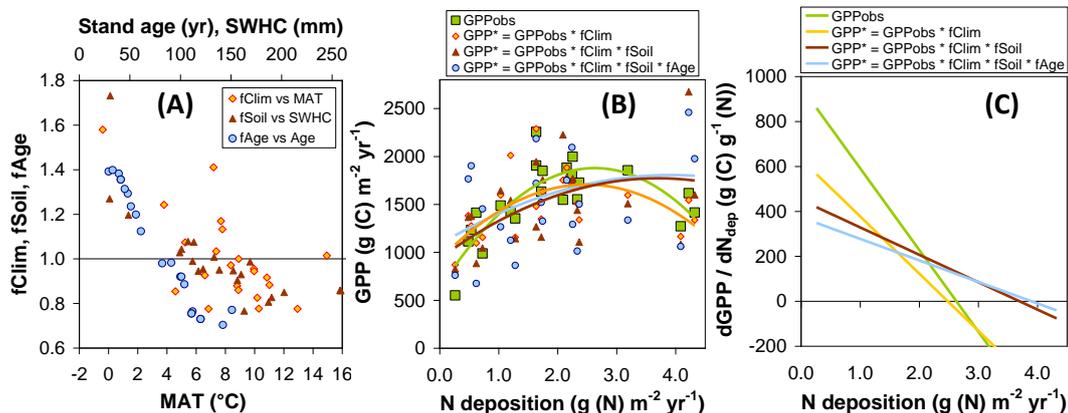
Figure 7. Model-based assessment of the sensitivity of gross primary productivity (GPP) to climate, soil, age and N_r deposition. (A) GPP standardization factors for observational (EC-based) data as a function of the dominant climatic and soil drivers (MAT: mean annual temperature; SWHC: soil water holding capacity; see text for details); (B) the resulting standardized GPP* compared with the original GPP$_{obs}$ as a function of N_{dep} (one data point for each of 22 sites), with 2nd-order polynomial fits; (C) estimates of the GPP response to N_{dep}, calculated as the slope of the tangent line to the quadratic fits and plotted as a function of N_{dep}.
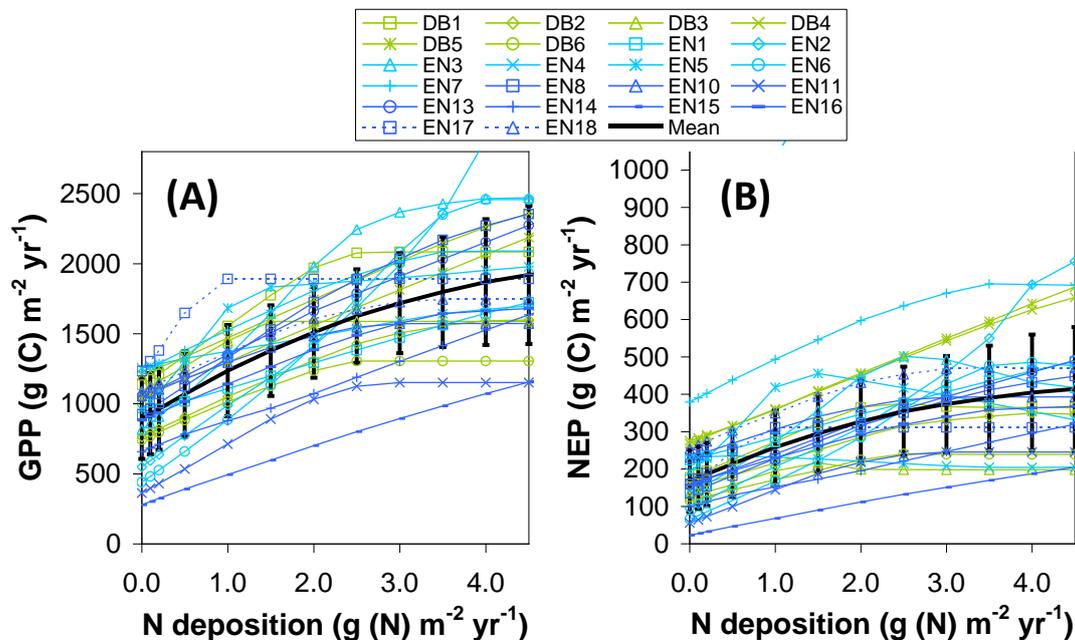
Figure 8. Modelling (BASFOR) sensitivity scenarios for (A) gross primary productivity (GPP) and (B) net ecosystem productivity (NEP) for 22 forest sites (with mean +/- standard deviation), in which each site was modelled using a range of N_{dep} values from 0 to 4.5 g (N) m^{-2} yr^{-1} (constant N_{dep} over the lifetime of the stands).
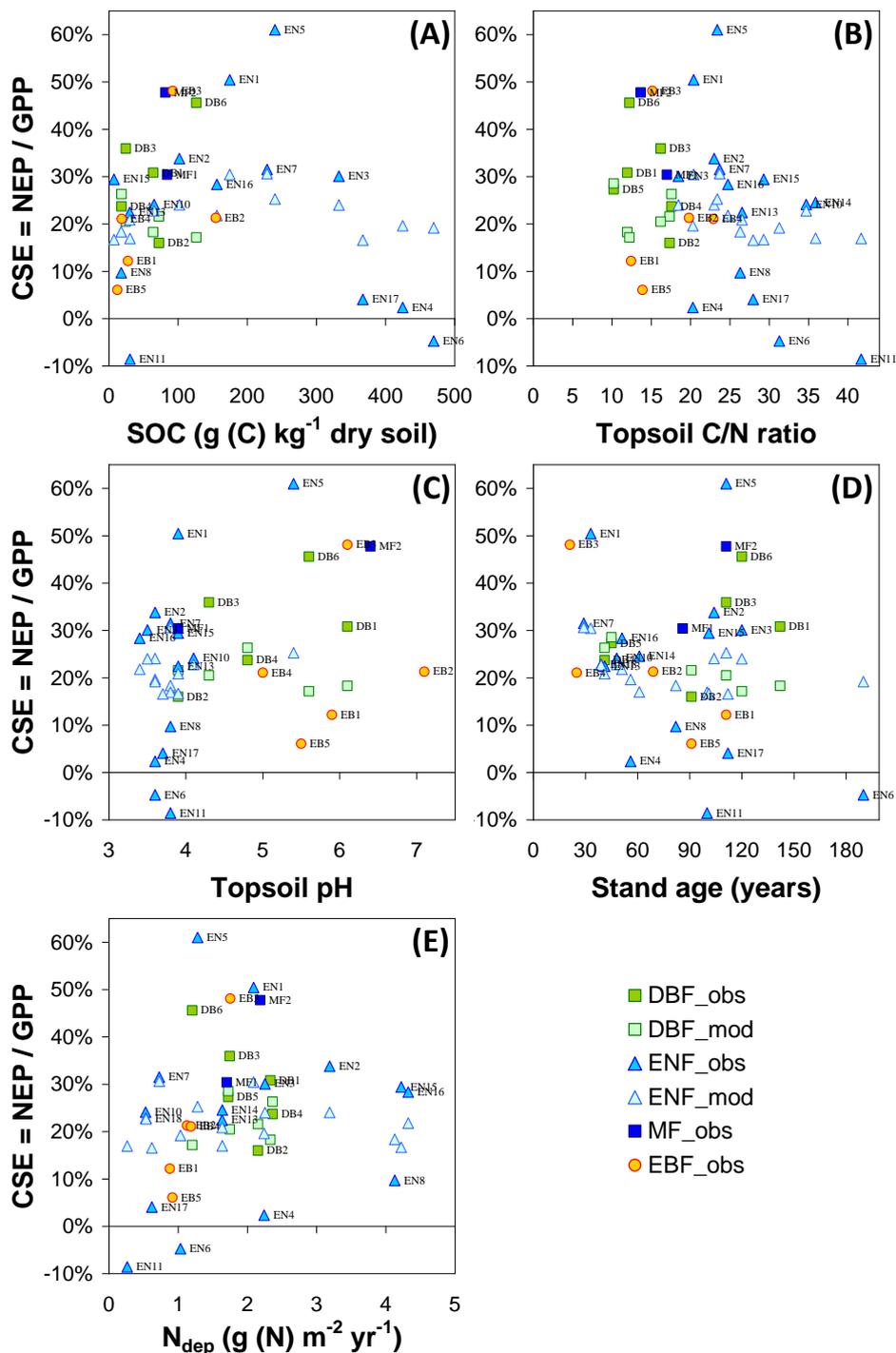
Figure 9. Variability of observation-based (obs) and modelled 5-yr (mod) carbon sequestration efficiency defined as the NEP/GPP ratio calculated over the ~5-yr measurement period, plotted as a function of (A) topsoil organic carbon content, (B) topsoil C/N ratio, (C) topsoil pH, (D) forest stand age, and (E) nitrogen deposition. DBF: deciduous broadleaf forests; ENF: coniferous evergreen needleleaf forests; MF: mixed needleleaf/broadleaf forests; EBF: Mediterranean evergreen broadleaf forests.
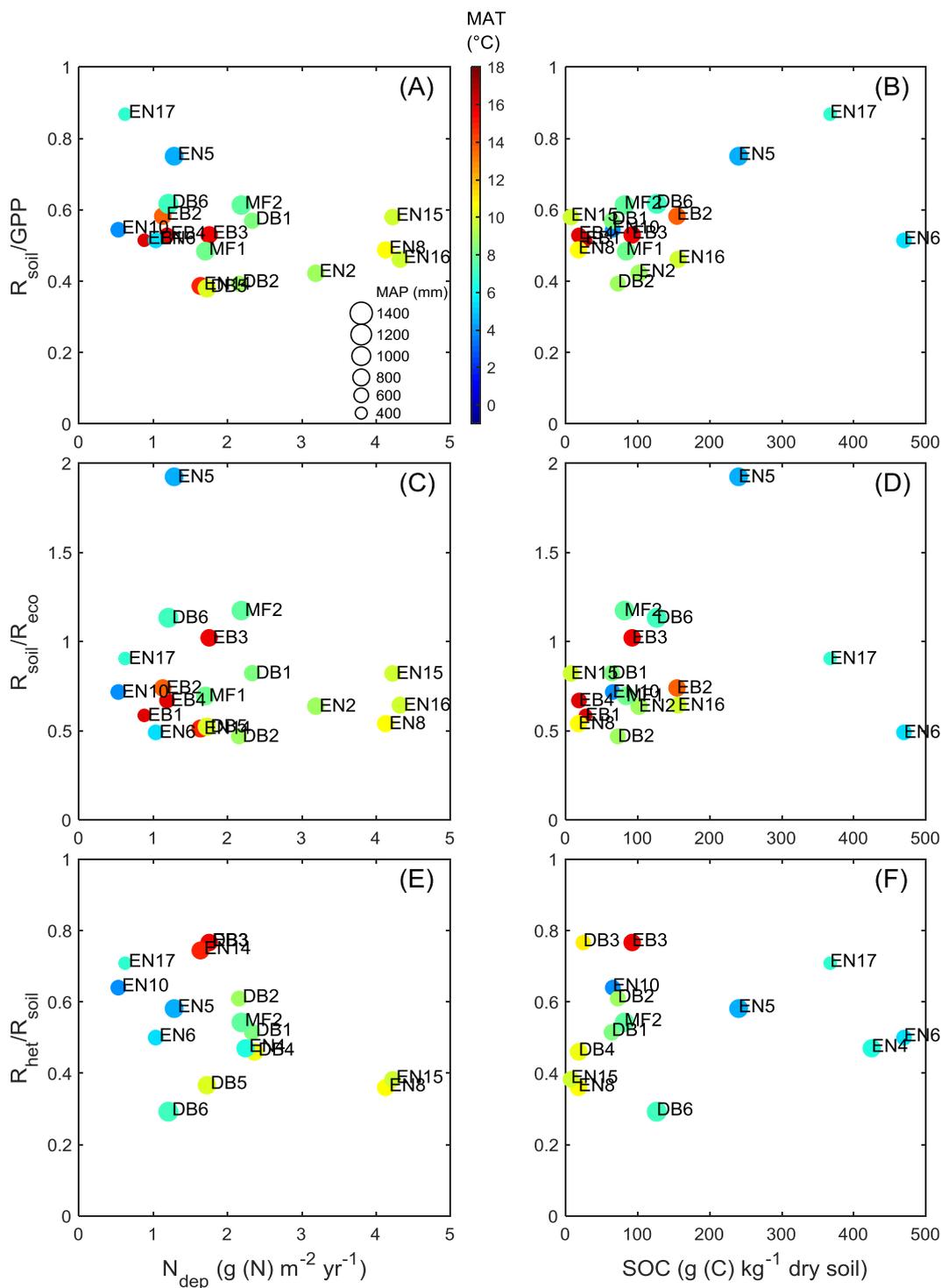
Figure 10. Variability of normalized soil respiration metrics as a function of nitrogen deposition (A, C, E) and soil organic carbon (B, D, F). In all plots, the color scale indicates mean annual temperature (MAT), and the symbol size is proportional to mean annual precipitation (MAP).

Table 1. BASFOR model state variables, inputs and outputs, and other acronyms used in the study.

BASFOR variables	Description
Tree state variables	
CL	Carbon pool in Leaves
CB	Carbon pool in Branches
CS	Carbon pool in Stems
CLBS	Carbon pool in Leaves, Branches and Stems
CR	Carbon pool in Roots
CRES	Carbon pool in Reserves
NL	Nitrogen pool in Leaves
SD	Forest stand density
Soil state variables	
CLITT	Carbon pool in Litter layers
CSOMF	Carbon pool in Soil Organic Matter (Fast turnover)
CSOMS	Carbon pool in Soil Organic Matter (Slow turnover)
NLITT	Nitrogen pool in Litter layers
NSOMF	Nitrogen pool in Soil Organic Matter (Fast turnover)
NSOMS	Nitrogen pool in Soil Organic Matter (Slow turnover)
NMIN	Soil Mineral (inorganic) Nitrogen pool
WA	Water pool in the root zone
Soil parameters	
Φ_{SAT}	Saturation soil water content
Φ_{FC}	Field capacity
Φ_{WP}	Wilting point
ROOTD	Root depth
Model inputs (daily time step)	
R_g	Daily global radiation
T_a	Daily average air temperature
P	Daily accumulated rain
WS	Daily average wind velocity
RH	Water vapour pressure
CO_2	Annual mean CO_2 mixing ratio
N_{dep}	Annual atmospheric nitrogen deposition
thinFR	Fraction of trees removed by thinning
Model outputs	
H	Tree height
DBH	Diameter at breast height
LAI	Leaf area index
LeafN	Leaf N content
GPP	Gross primary productivity
R_{eco}	Ecosystem respiration
R_{het}	Soil heterotrophic respiration
NPP	Net primary productivity
NEE	Net ecosystem exchange
ET	Evapotranspiration
N_{miner}	Nitrogen supply from SOM mineralization
N_{upt}	Root N uptake by trees
N_{leach}	Inorganic N leaching
NO	Nitric oxide
N_2O	Nitrous oxide
$N_{emission}$	Gaseous soil NO + N_2O emissions

Other variables	
GPP_{obs}, NEP_{obs}	Observation-based (eddy covariance) GPP or NEP
GPP_{base}	Baseline model run for GPP
GPP*, NEP*	Model-standardized observation-based GPP or NEP
f_{CLIM}, f_{SOIL}, f_{AGE}	Model-derived standardization factors to account for climate, soil, age
NECB	Modelled net ecosystem carbon balance, calculated as d(CLBS+CR+CSOM+CLITT)/dt
R_{aut}	Autotrophic respiration
R_{soil}	Soil (heterotrophic and rhizospheric) respiration
SCE	Soil CO_2 efflux measured by chamber methods
CSE_{obs}	Observation-based carbon sequestration efficiency (NEP_{obs}/GPP_{obs})
$CSE_{5-yr, lifetime}$	Modelled carbon sequestration efficiency; = NEP/GPP (5-yr), or NECB/GPP (lifetime)
NUE	Modelled nitrogen use efficiency, calculated as N_{upt} / N_{supply}
N_{supply}	Total mineral N supply, calculated as (modelled) N_{miner} + (observation-based) N_{dep}
N_{loss}	Modelled percentage ecosystem N losses, calculated as (N_{leach} + $N_{emission}$) / N_{supply}
dC/dN, $dGPP/dN_{dep}$, $dNEP/dN_{dep}$	Response (slope) of ecosystem C productivity versus atmospheric N_r deposition
SWHC	Soil water holding capacity, = (Φ_{FC} - Φ_{WP}) x ROOTD
MAT, MAP	Mean annual temperature or precipitation
CEXP	Carbon exported by thinning or harvest in forests

Table 2. Estimates of ecosystem dC/dN response for gross and net productivity, calculated under different assumptions and expressed as g (C) photosynthesized or sequestered per g (N) deposited from the atmosphere. The stepwise method described in this paper (for forests only) first calculates $dGPP/dN_{dep}$ for both raw GPP_{obs} and GPP^* standardized by meta-modelling following Eq. (10)-(17); this is then multiplied by different estimates of CSE (from observations or from modelling) to provide an NEP (5-yr) or NECB (lifetime) equivalent. Quadratic regressions (Q) are used for productivity vs N_{dep}, whereby the mean tangent slope is calculated either over the whole N_{dep} range (0-4.3 g (N) m^2 yr^{-1}) (italics), or discarding sites with N_{dep} larger than 2.5 g (N) m^2 yr^{-1} (bold). Uncertainty ranges are calculated from combined standard errors in $dGPP/dN_{dep}$ and in CSE. For comparison purposes only, are also displayed i) simple linear regression (L) slopes of EC-based (not standardized) GPP_{obs} and NEP_{obs} versus N_{dep} for both forests and semi-natural vegetation; and ii) results of the meta-modelling standardization method applied directly to NEP_{obs} instead of GPP_{obs}.

	FORESTS						SEMI-NATURAL
				GPP*			
	GPP_{obs}	GPP_{obs} x f_{CLIM}	GPP_{obs} x f_{CLIM} x f_{SOIL}	GPP_{obs} x f_{CLIM} x f_{SOIL} x f_{AGE}			GPP_{obs}
Gross primary productivity per unit N_{dep} $dGPP/dN_{dep}$							
(g (C) g^{-1} (N))	260 [38, 483] (M,Q) **425 [203, 648]** (M,Q) 146 [89, 203] (A,L) **432 [355, 509]** (A,L)	146 [-121, 412] (M,Q) **261 [-5, 528]** (M,Q)	218 [-174, 609] (M,Q) **273 [-119, 664]** (M,Q)	190 [-375, 755] (M,Q) **234 [-331, 799]** (M,Q)			374 [275, 474] (A,L) **504 [331, 677]** (A,L)
CSE_{obs} * (dGPP /dN_{dep})	64 [8, 136] (M,Q) **105 [43, 182]** (M,Q)	36 [-25, 116] (M,Q) **64 [-1, 149]** (M,Q)	53 [-36, 172] (M,Q) **67 [-25, 187]** (M,Q)	47 [-79, 213] (M,Q) **57 [-69, 225]** (M,Q)			
CSE_{5-yr} * (dGPP /dN_{dep})	57 [8, 110] (M,Q) **93 [42, 147]** (M,Q)	32 [-25, 94] (M,Q) **57 [-1, 120]** (M,Q)	47 [-36, 138] (M,Q) **59 [-25, 151]** (M,Q)	41 [-78, 172] (M,Q) **51 [-69, 181]** (M,Q)			
$CSE_{lifetime}$ * (dGPP /dN_{dep})	47 [7, 91] (M,Q) **77 [35, 122]** (M,Q)	26 [-21, 78] (M,Q) **47 [-1, 100]** (M,Q)	39 [-30, 115] (M,Q) **49 [-20, 125]** (M,Q)	34 [-65, 143] (M,Q) **42 [-57, 151]** (M,Q)			
	NEP_{obs}	NEP_{obs} x f_{CLIM}	NEP* NEP_{obs} x f_{CLIM} x f_{SOIL}	NEP_{obs} x f_{CLIM} x f_{SOIL} x f_{AGE}			NEP_{obs}
Net ecosystem productivity per unit N_{dep} dNEP /dN_{dep}							
(g (C) g^{-1} (N))	108 [-118, 333] (M,Q) **178 [-47, 403]** (M,Q) 71 [29, 114] (A,L) **224 [157, 292]** (A,L)	93 [-166, 352] (M,Q) **161 [-98, 420]** (M,Q)	120 [-162, 403] (M,Q) **165 [-117, 447]** (M,Q)	112 [-146, 370] (M,Q) **146 [-112, 404]** (M,Q)			89 [46, 132] (A,L) **34 [-41, 109]** (A,L)

GPP: gross primary productivity; NEP: net ecosystem productivity; NECB: net ecosystem carbon balance
GPP_{obs}, NEP_{obs}: observation-based (eddy covariance) GPP or NEP
GPP^*, NEP^*: GPP or NEP standardized through meta-modelling for the effects of climate (f_{CLIM}), soil (f_{SOIL}), age (f_{AGE})
CSE: carbon sequestration efficiency
CSE_{obs} = NEP_{obs} / GPP_{obs} (eddy covariance-based, mean value across all sites)
CSE_{5-yr} = NEP_{5-yr} / GPP_{5-yr} (BASFOR model-based over 5-yr period, mean value across all sites)
$CSE_{lifetime}$ = $NECB_{lifetime}$ / $GPP_{lifetime}$ (BASFOR model-based over lifetime, mean value across all sites)
Q: calculated by quadratic regression
L: calculated by simple linear regression
A: calculated on the basis of all sites in the monitoring network (31 forests, 9 semi-natural sites)
M: calculated on the basis of the subset of 22 forest sites included in BASFOR meta-modelling